

Concealed Quantum Telecomputation for Anonymous 6G URLLC Networks

Fakhar Zaman, *Student Member, IEEE*, Saw Nang Paing, Ahmad Farooq, Hyundong Shin[✉], *Fellow, IEEE*, and Moe Z. Win[✉], *Fellow, IEEE*

Abstract—Distributed learning and multi-tier computing are the key ingredients to ensure ultra-reliable and low-latency communication (URLLC) in 6G networks. The distinct transition from connected things in 5G URLLC networks to connected intelligence in 6G URLLC networks requires ultra-secure communication due to the massive amount of private data. However, it is a challenging task to ensure stringent 6G URLLC requirements along with user privacy and data security in distributed networks. In this paper, we devise a distributed quantum computation protocol to perform a nonlocal controlled unitary operation on a bipartite input state in concealed and counterfactual manner and integrate it with anonymous quantum communication networks. This distributed protocol allows Bob to apply an arbitrary singlequbit unitary operator on Alice's qubit in a controlled and probabilistic fashion, without revealing the operator to her and without transmitting any physical particle over the quantum channel-called the counterfactual concealed telecomputation (CCT). It is shown that the CCT protocol neither requires the preshared entanglement nor depends on the bipartite input state and that the single-qubit unitary teleportation is a special case of CCT. The quantum circuit for CCT can be implemented using the (chained) quantum Zeno gates. The protocol becomes deterministic with simplified circuit implementation if the initial composite state of Alice and Bob is a Bell-type state. Furthermore, we provide numerical examples of quantum anonymous broadcast networks using the CCT protocol and show their degrees of anonymity in the presence of malicious users.

Index Terms—6G, blind quantum computation, counterfactual quantum communication, distributed learning, quantum anonymous networks, ultra-reliable and low-latency communication.

I. INTRODUCTION

PROLIFERATION of time-, mission- and privacy-critical applications comes with the vast demand of ultra-high security and ultra-reliable and low-latency communication

Manuscript received 22 October 2022; revised 31 January 2023; accepted 7 March 2023. Date of publication 29 May 2023; date of current version 6 July 2023. The fundamental research described in this paper was supported in part by the National Research Foundation of Korea (NRF) grant funded by the Korean government (MSIT) (No. 2019R1A2C2007037 and 2022R1A4A3033401), by the MSIT (Ministry of Science and ICT), Korea, under the ITRC (Information Technology Research Center) support program (IITP-2021-0-02046) supervised by the IITP (Institute for Information & Communications Technology Planning & Evaluation) and in part by the National Science Foundation under Grant CCF-2153230. (*Corresponding author: Hyundong Shin.*)

Fakhar Zaman is with the Department of Electronics and Information Convergence Engineering, Kyung Hee University, Yongin 17104, South Korea, and also with the Wireless Information and Network Sciences Laboratory, Massachusetts Institute of Technology, Cambridge, MA 02139 USA.

Saw Nang Paing, Ahmad Farooq, and Hyundong Shin are with the Department of Electronics and Information Convergence Engineering, Kyung Hee University, Yongin 17104, South Korea (e-mail: hshin@khu.ac.kr).

Moe Z. Win is with the Laboratory for Information and Decision Systems, Massachusetts Institute of Technology, Cambridge, MA 02139 USA (e-mail: moewin@mit.edu).

Color versions of one or more figures in this article are available at <https://doi.org/10.1109/JSAC.2023.3280989>.

Digital Object Identifier 10.1109/JSAC.2023.3280989

(URLLC) across 6G and beyond wireless networks. It is envisioned that the data rate in 6G networks will be enhanced up to 1 Terabit to meet 99.99999% (7 nines) reliability and 1-millisecond end-to-end latency requirements. In recent years, deep learning, deep reinforcement learning, and distributed learning have been demonstrated as key elements in the achievability of stringent 6G URLLC requirements [1], [2], [3]. Despite the advantages of deep learning and deep reinforcement learning in wireless communications, the curse of dimensionality and the highly dynamic nature of emerging networks significantly reduce the learning rate of the system, which may violate stringent 6G URLLC requirements. Furthermore, many network applications face resource-constraint problems. In these scenarios, multi-tier computing (from cloud to edge) and distributed learning can significantly enhance the learning rate of the system.

The recent developments in multi-tier computing and distributed learning play a vital role in the achievability of the 6G URLLC. However, it makes the user identity and the data security vulnerable to cyberattacks. Concealing the identity of users and preserving the security of data are the fundamental concerns in 6G networks. Recently, federated learning has shown the potential to ensure the data security with an enhanced learning rate [3], [4]. However, the computational overhead limits the efficiency of algorithms. Furthermore, the development of quantum computers imposes a threat to classical cryptography systems. These limitations make it challenging to ensure stringent 6G URLLC requirements along with *user privacy* and *data security*.

Quantum communication and computation provide novel ways of secure communication and private distributed learning with no counterpart in classical networks. In particular, quantum anonymous communication addresses the connectivity issues such as the security of private data and the anonymity of users in wireless networks [5], [6], [7], whereas, blind quantum computation allows one party to use quantum computational resources of a remote party without revealing input data, computation, and output data [8], [9], [10], [11], [12]. Due to the rising demand for secure 6G URLLC networks, quantum anonymous communication paves the way towards ultra-secure wireless networks while concealing the identities of the sender and the receiver under unconditional security. Quantum anonymity along with blind quantum computation provides an additional layer of security and privacy in distributed learning and wireless networking. In this paper, we propose a new type of distributed quantum computation to perform a nonlocal controlled unitary operation on a distinct party in a concealed manner and integrate it with quantum anonymity for 6G URLLC networks.

Nonlocal controlled unitary operators are one of the fundamental building blocks in distributed quantum computing [13], [14], [15] and quantum communications [16], [17], [18]. Recently, it has been shown that any bipartite nonlocal unitary operation on a $d_A \times d_B$ dimensional quantum system can be implemented using at most $4d_B - 5$ nonlocal controlled unitary operators, regardless of d_A , where d_A and d_B denote the dimensions of target and control quantum systems possessed by the remote parties Alice and Bob, respectively [19]. In particular, a two-qubit nonlocal controlled unitary operator plays an important role in distributed quantum computing as any n -qubit nonlocal unitary operation can be decomposed into a product of two-qubit nonlocal controlled unitary operators and single-qubit local operations [19], [20].

In general, a two-qubit controlled unitary operator can be represented as $U_c = I \otimes |0\rangle\langle 0| + U \otimes |1\rangle\langle 1|$, where I is the identity operator, U is an arbitrary single-qubit unitary operator, and \otimes denotes the Kronecker product. To devise a two-qubit nonlocal controlled unitary operator, U_c can be further decomposed to [21], [22]

$$U_c = (A_1 \otimes B_1) \left(\sum_{kl} e^{i\epsilon_{kl}\theta} |kl\rangle\langle kl| \right) (A_2 \otimes B_2), \quad (1)$$

where $\epsilon = \sqrt{-1}$; $|k\rangle$ and $|l\rangle$ denote the computational basis of target and control qubits; and A_i and B_i respectively are Alice's and Bob's single-qubit local unitary operators that depend on U . The implementation of two-qubit nonlocal controlled unitary operators has been accomplished using entanglement-assisted local operations and classical communication (LOCC) [21]. Such implementation requires: i) the knowledge of U at both Alice and Bob; and ii) a sufficient amount of preshared entanglement [21]. The goal of this paper is to demonstrate the implementation of a two-qubit nonlocal controlled unitary operation in a counterfactual manner without the aforementioned requirements.

Counterfactual quantum communication [23], [24], [25], [26], [27], [28] is a unique capability enabled by quantum mechanics, which allows remote parties to communicate information without transmitting any physical particle. To transmit classical information, the sender controls the presence and absence of an absorptive object (AO) in the interferometer in a classical manner. In recent years, it has been shown that the counterfactual communication is the application of the quantum Cheshire Cat effect, which states that the properties of the physical particle can be affected by external actions even if the physical particle is not present there [28]. Furthermore, since the measurement collapse the state of the quantum system, it has been shown that the quantum Cheshire Cat effect and the measurement frequency carry information in counterfactual communication [27], [28].

In quantum mechanics, the quantum Zeno (QZ) and chained QZ (CQZ) gates form a set of basic building blocks of counterfactual quantum communication and computation [29], [30], [31], [32], [33], [34], [35], [36], [37]. Although one can transmit classical information by controlling an AO in a classical manner, the communication achieved by using the

QZ gates is *semi-counterfactual*—that is, counterfactual for the presence of the AO only, whereas CQZ gates ensure the *full counterfactuality* of quantum protocols [28], [38], [39]. Recently, a full-duplex communication protocol has been presented to exchange one-bit classical information in a counterfactual manner by using a quantum AO and modified QZ (MQZ) gates [40], [41]. The idea of counterfactual full-duplex communication has been extended to transmit one-qubit quantum information in each direction [41], [42], [43], using the so-called *counterfactual swap gate*, which is a special case of distributed quantum computing in a bipartite system. In addition to quantum communication [41], [42], [44], [45] and cryptography [46], [47], [48], [49], [50], [51], the counterfactuality has been introduced in distributed computation by using the counterfactual CNOT gate [52], [53]. However, these distributed computation protocols require the knowledge of U at both Alice and Bob to perform a controlled unitary operation, similar to the entanglement-assisted LOCC algorithms.

We propose a new type of distributed quantum computation protocols, which enables one party, say Bob, to apply two-qubit controlled unitary operator U_c on a two-qubit bipartite state in a probabilistic, concealed, and counterfactual manner without revealing the operator U to Alice and without transmitting any physical particle over the quantum channel. The main advantage of the proposed algorithms over the existing techniques [52], [53] is the concealed behavior of the unitary operation, which can play an important role in cryptographic tasks. The proposed protocols are accomplished by decomposing the two-qubit controlled unitary operator corresponding to U into global controlled flipping operations and single-qubit local operations at the remote parties. The key features of this protocol are that i) the global controlled flipping operations are implemented in a counterfactual way, and ii) both the global operations and Alice's local operations are implemented in a way that U is concealed from Alice. This protocol is called *counterfactual concealed telecomputation (CCT)*. The counterfactual implementation of global controlled flipping is demonstrated by using the QZ and CQZ gates where Alice's qubit acts as a quantum AO to ensure the counterfactuality of the protocol, whereas Bob's qubit is encoded in the polarization degree of the photon. It is shown that the single-qubit unitary teleportation is a special case of CCT and the protocol is accomplished independent of the bipartite input state without using the preshared entanglement. If the composite state of Alice and Bob is a Bell-type state, the protocol becomes deterministic and the quantum circuit for CCT can be simplified significantly.

The remaining sections are organized as follows. Section II-B addresses secure intelligence and anonymity in 6G URLLC networks. Section III briefly introduces QZ, CQZ, dual CQZ (D-CQZ), MQZ dual MQZ (D-MQZ), distributed controlled flipping (DCF) and dual DCF (D-DCF) gates for general input states. In Section IV, the CCT is proposed to implement a two-qubit controlled unitary operator on an arbitrary unknown input state using the D-DCF gates. The deterministic CCT protocol is further proposed for Bell-type

input states using the DCF gates. Finally, Section V gives conclusions and future works.

II. 6G SECURITY

It is envisioned that 6G wireless networks will enable emerging technologies such as autonomous driving, industry automation, and three-dimensional mapping and localization. These new technologies require ultra-high reliability, ultra-low latency, and ultra-high security, which make it challenging to realize 6G networks. This section briefly overview challenges in 6G security followed by the quantum-secure intelligence for URLLC networks.

A. Challenges

In wireless communication networks, ultra-high reliability is required for life-threatening circumstances whereas ultra-low latency ensures real-time functionality in time-critical applications [54], [55], [56]. In addition, communication security is a pivotal issue in URLLC networks. Maintaining security under the stringent URLLC constraints in networks is a challenging task as it requires a delicate balance between eavesdropping detection capabilities and performances. Furthermore, the ever-increasing number of participating nodes and the highly dynamic nature of 6G networks make it even more challenging to ensure security and stringent URLLC requirements at the same time [57]. These constraints require scalable and efficient algorithms and robust implementation of security mechanisms.

One of the major bottlenecks to ensuring stringent URLLC requirements in secure wireless networks is the time required to encrypt and decrypt secret information, which may violate the stringent low latency requirements. Although physical layer security can provide an alternate solution, the secrecy metrics are not applicable to evaluate the performance in 6G networks due to the finite block-length requirement to ensure URLLC [58], [59]. In this scenario, quantum communication provides novel ways of information-theoretic secure communication with the capability of eavesdropping detection, which has no counterpart in classical communication. This unconditional security and robust communication rely on fundamental laws of quantum physics such as the quantum entanglement, nonlocality, and no-cloning theorem [60], [61], [62], [63]. This article puts forth quantum telecomputation protocols based on single-particle non-locality and simulates the proposed algorithms for anonymous networks.

B. Quantum-Secure Intelligence and Anonymity

Private distributed learning studies the interplay between user privacy, data security, and machine learning, which is of crucial importance in data-intensive applications. Indeed in many collaborative learning methodologies, such as federated learning, it is highly desirable that the privacy and security of the users and the data are preserved, respectively [3], [4]. However, ensuring the stringent URLLC requirements along with user privacy and data security is one of the main challenges in the development of 6G URLLC networks. In this

section, we briefly introduce the quantum anonymous communication followed by quantum anonymity achieved by the private information retrieval protocol for distributed networks.

In wireless communication systems, anonymity is defined as the confidentiality of participating users, which allows both the sender and receiver to transmit and receive information without revealing their identities. The idea of anonymity has been used in quantum as well as classical networks [6], [7]. Recently, the quantum anonymous private information retrieval (QAPIR) protocol has been proposed by integrating anonymity with quantum secure communication to ensure the security and privacy of the transmitted data and participating users in the network, respectively [5]. The quantum anonymous broadcast network is one of the key ingredients to establishing the QAPIR protocol, which allows any user s to broadcast classical information anonymously by using the shift operator $U_{(s)}$. In addition, the QAPIR protocol relies on the quantum anonymous entanglement generation and quantum anonymous entanglement verification protocols. These protocols require preshared $(n + 1)$ -partite d -dimensional Greenberger-Horne-Zeilinger (GHZ) states, where n denotes the number of users in the network. The security of quantum communication and computation can be compromised by counterfactual attacks such as the counterfactual man-in-the-middle attack. In this scenario, counterfactual quantum communication and computation has the potential to ensure the security of private data and meet the stringent URLLC requirements in 6G networks in the following manners.

- 1) One of the bottlenecks in quantum anonymity and blind quantum computation protocols is the hidden assumption of a shared phase reference between participating nodes, i.e.—*the existence of common definitions of quantum superposition states and non-diagonal Hamiltonian evolution* [64], [65]. The absence of this shared phase reference introduces unwanted errors in communication/computation tasks and may violate the stringent ultra-reliability requirements of the 6G networks. In counterfactual quantum communication, as no physical particle is transmitted over the quantum channel, only local operations are applied on qubits. Hence, legitimate parties can perform the desired task in the absence of the shared phase reference without any qubit error with enhanced reliability.
- 2) It is already well known that quantum communication provides unique ways of secure communication with no counterpart in classical communication [60], [62], [66], [67], [68], [69], [70]. However, it has been shown that counterfactual attacks threaten conventional quantum cryptography protocols and the eavesdropper may access the secret information without being detected. In this scenario, counterfactual quantum cryptography has the potential to provide security against counterfactual attacks [71].

The CCT protocol can play an important role in quantum-enabled federated learning and quantum secure communication systems. For instance (see Fig. 1), we demonstrate the degree of anonymity for the quantum anonymous broadcast network with the CCT protocol in Section IV-D.

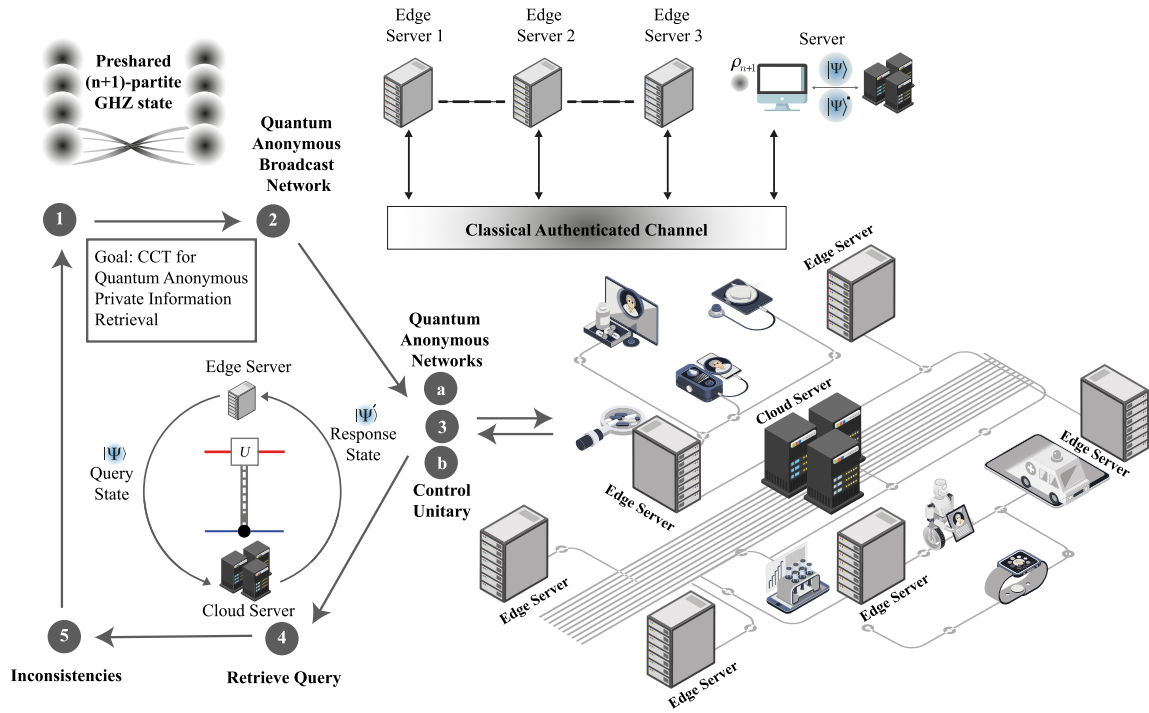


Fig. 1. An anonymous 6G URLLC network with the CCT protocol. The cloud server starts the protocol by preparing a GHZ state followed by the Edge servers execute the counterfactual controlled unitary operation to anonymously broadcast their classical information.

III. COUNTERFACTUAL QUANTUM GATES

For the sake of completeness, we briefly introduce fundamental gates for general input states such as QZ, CQZ, MQZ, DCF gates, and their dual forms in [41], which are used in counterfactual quantum communication and computation. To perform communication and computation tasks in a counterfactual manner, only the control terminal of these gates interacts with a classical or quantum AO.

A. Quantum Gates

In classical computing, logic gates are building blocks of digital circuits. Most of the logic gates are irreversible in classical mechanics. In contrast, quantum gates are reversible and allow classical computing using reversible quantum gates. For instance, all Boolean functions can be implemented by using a reversible Toffoli gate at the cost of ancillary qubits. Table I shows the most widely used gates in quantum mechanics with their gate symbols and matrix representations. For instance, the Pauli- x gate X is equivalent to the classical NOT gate and transforms

$$|\psi\rangle = \alpha \begin{bmatrix} 1 \\ 0 \end{bmatrix} + \beta \begin{bmatrix} 0 \\ 1 \end{bmatrix} = \begin{bmatrix} \alpha \\ \beta \end{bmatrix} \quad (2)$$

as $\alpha|1\rangle + \beta|0\rangle$ where $|\alpha|^2 + |\beta|^2 = 1$. In general, the quantum gates are represented by a unitary operator $U = \exp(-i\mathcal{H}t/\hbar)$ and transform the state of a quantum system as (governed in Schrodinger's equation)

$$i\hbar \frac{\partial |\psi\rangle}{\partial t} = \mathcal{H} |\psi\rangle, \quad (3)$$

where \hbar is the Planck constant and \mathcal{H} is the Hamiltonian of the quantum gate. For a single qubit system, a unitary

operator U is a 2×2 matrix and can be decomposed into the product of three rotation matrices as follows:

$$U = R_z(\phi) R_y(\theta) R_z(\varphi), \quad (4)$$

where ϕ , θ , and φ are the Euler angles and

$$R_y(\theta) = \begin{bmatrix} \cos(\theta/2) & -\sin(\theta/2) \\ \sin(\theta/2) & \cos(\theta/2) \end{bmatrix}, \quad (5)$$

$$R_z(\varphi) = \begin{bmatrix} e^{-i\varphi/2} & 0 \\ 0 & e^{i\varphi/2} \end{bmatrix}. \quad (6)$$

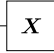
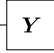
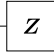
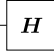
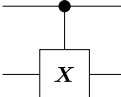
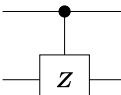
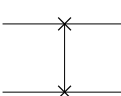
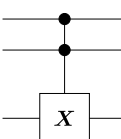
With $b \in \mathbb{Z}_2 = \{0, 1\}$, we use for convenience

$$R_y(\theta; b) = \begin{cases} R_y(\theta), & \text{if } b = 0, \\ R_y(-\theta), & \text{if } b = 1. \end{cases} \quad (7)$$

B. QZ Effect

Zeno's paradox is a philosophical problem presented by the Greek philosopher Zeno of Elea, which states that the motion of an object in a vanishingly small time interval approaches zero. An effect is often paraphrased as—*a watched kettle never boils*. Although Zeno's paradox was solved in later years by physicists with the invention of laws of motion, quantum mechanics arises an entirely new paradox—called the *QZ effect*. This effect—also known as Turing's paradox—describes the time evolution of a quantum system under repeated measurements [72], [73], [74]. The Turing paradox states that *if the initial state of a system is prepared in the eigenstate of an arbitrary observable and the measurements are performed with frequency N , the probability that the state of the system remains unchanged approaches one as N goes to infinity*. For instance, assume that the state of a closed

TABLE I
ELEMENTARY QUANTUM GATES

Operator	Gate	Matrix
Pauli- x		$\mathbf{X} = \begin{bmatrix} 0 & 1 \\ 1 & 0 \end{bmatrix}$
Pauli- y		$\mathbf{Y} = \begin{bmatrix} 0 & -i \\ i & 0 \end{bmatrix}$
Pauli- z		$\mathbf{Z} = \begin{bmatrix} 1 & 0 \\ 0 & -1 \end{bmatrix}$
Hadamard		$\mathbf{H} = \frac{1}{\sqrt{2}} \begin{bmatrix} 1 & 1 \\ 1 & -1 \end{bmatrix}$
Controlled-NOT		$\text{CNOT} = \begin{bmatrix} 1 & 0 & 0 & 0 \\ 0 & 1 & 0 & 0 \\ 0 & 0 & 0 & 1 \\ 0 & 0 & 1 & 0 \end{bmatrix}$
Controlled- Z		$\text{CPHASE} = \begin{bmatrix} 1 & 0 & 0 & 0 \\ 0 & 1 & 0 & 0 \\ 0 & 0 & 1 & 0 \\ 0 & 0 & 0 & -1 \end{bmatrix}$
Swap		$\text{SWAP} = \begin{bmatrix} 1 & 0 & 0 & 0 \\ 0 & 0 & 1 & 0 \\ 0 & 1 & 0 & 0 \\ 0 & 0 & 0 & 1 \end{bmatrix}$
Toffoli		$\mathbf{T} = \begin{bmatrix} \mathbf{I}_{6 \times 6} & \mathbf{0}_{6 \times 2} \\ \mathbf{0}_{2 \times 6} & \mathbf{X} \end{bmatrix}$

quantum system at $t = t_0$ is $|\psi(t_0)\rangle = |\psi_0\rangle$ where $|\psi_0\rangle$ is an eigenstate of an arbitrary observable. Then, the state of the system undergoes a unitary evolution as follows:

$$\begin{aligned} |\psi(t)\rangle &= \mathbf{U}(t) |\psi_0\rangle \\ &= e^{-i\mathcal{H}t/\hbar} |\psi_0\rangle \end{aligned} \quad (8)$$

with $t_0 = 0$ where $|\psi(t)\rangle$ denotes the state of the system at time $t > t_0$ and \mathcal{H} is the Hamiltonian of the given system. The probability that the system remains unchanged at time instant t is given as [75]

$$\begin{aligned} p(t) &= |\langle \psi_0 | e^{-i\mathcal{H}t/\hbar} | \psi_0 \rangle|^2 \\ &\approx 1 - (\Delta\mathcal{H})^2 t^2, \end{aligned} \quad (9)$$

where

$$\Delta\mathcal{H} = \sqrt{\langle \psi_0 | \mathcal{H}^2 | \psi_0 \rangle - \langle \psi_0 | \mathcal{H} | \psi_0 \rangle^2}. \quad (10)$$

Now, if the measurement is performed with frequency N at regular intervals t/N , the probability that the system remains unchanged is given as [76]

$$p(t) \approx \left(1 - \frac{(\Delta\mathcal{H})^2 t^2}{N^2}\right)^N. \quad (11)$$

As $N \rightarrow \infty$, this probability goes to one. Hence, if the time interval between the repeated measurements is vanishingly small, it freezes the time evolution of the quantum system.

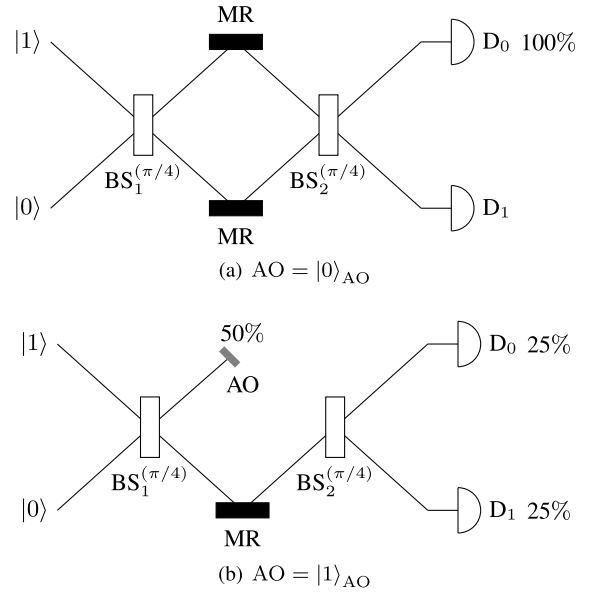


Fig. 2. EV-IFM. (a) In the absence of the AO, the detector D_0 clicks with certainty where MR stands for a mirror. (b) In the presence of the AO, unless the photon is absorbed by the AO, the detectors D_0 and D_1 click with equal probability.

In case no measurement is performed on the given quantum system, the state of the system keeps evolving and the state of the system transforms to $|\psi(t_N)\rangle = |\psi_N\rangle$. This phenomenon has been used in quantum mechanics to reduce the decay rate of an unstable quantum system by performing frequent measurements [29], [77], [78]. The decay rate of the quantum state depends on the frequency of repeated measurements. As the frequency of repeated measurements increases, the decay rate approaches zero. Under the asymptotic limits, the unstable quantum state collapses back to the initial state. Note that if the frequency of the measurements is very low but positive, it can enhance the decay rate of an unstable quantum system—known as the quantum anti-Zeno effect [79], [80], [81].

C. Interaction-Free Measurement

Quantum entanglement, which allows two distinct parties to instantaneously and deterministically know the state of each other even if they are thousands of miles apart, has become one of the intriguing aspects of quantum mechanics. Another manifestation of non-locality, known as the interaction-free measurement (IFM), allows determining the presence of an object in a certain region without interacting with it. The basic idea was first introduced in [82] and later extended in [83] (EV-IFM). However, the efficiency of EV-IFM is limited by 50%. In [30] (KW-IFM), the idea is further modified for making the fraction of IFM arbitrarily close to one.

1) *EV-IFM*: The EV-IFM is based on the Mach-Zehnder interferometer [83], [84], which uses two balanced beam splitters $\text{BS}^{(\pi/4)}$ and two detectors D_0 and D_1 (see Fig. 2).¹ Assume that $|0\rangle$ and $|1\rangle$ denote the presence of a photon

¹ $\text{BS}^{(\theta)}$ stands for a beam splitter with the transmissivity of $\sin^2 \theta$ and the reflectivity of $\cos^2 \theta$.

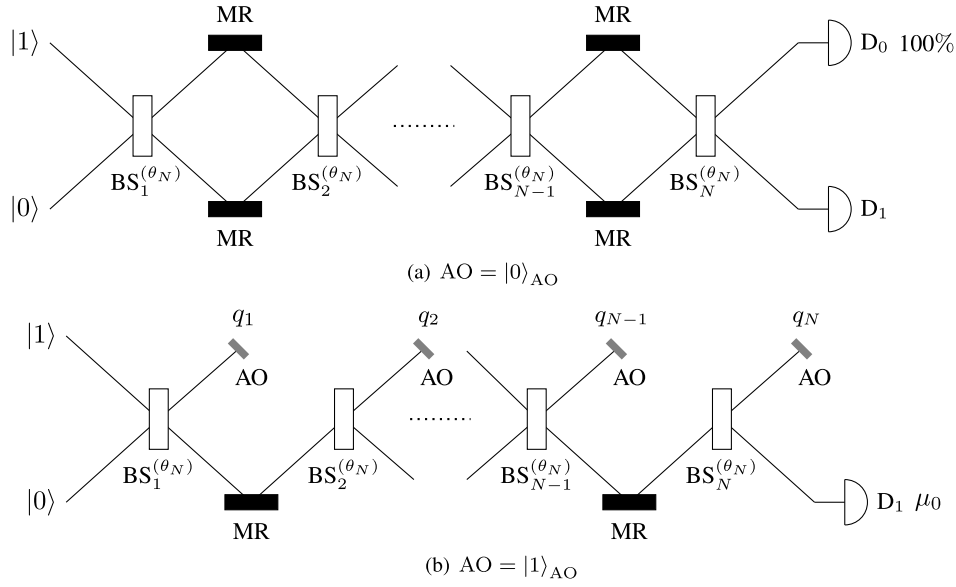


Fig. 3. KW-IFM. (a) In the absence of the AO, the detector D_0 clicks with certainty. (b) In the presence of the AO, the detector D_1 clicks unless the photon is absorbed by the AO with the probability μ_0 .

in the lower and upper paths, respectively. The protocol starts by initializing the photon in the state $|\psi_0\rangle = |0\rangle$. As illustrated in Fig. 2, when the photon reaches $BS_1^{(\pi/4)}$, the corresponding unitary operation $R_y(\pi/2)$ creates the balanced spatial superposition as follows:

$$\begin{aligned} |\psi_1\rangle &= R_y(\pi/2) |\psi_0\rangle \\ &= \frac{1}{\sqrt{2}} (|0\rangle + |1\rangle). \end{aligned} \quad (12)$$

To determine the existence of an object in the interferometer, assume that the photon is absorbed by the AO if it interacts with it. Let $|0\rangle_{AO}$ and $|1\rangle_{AO}$ denote the absence and presence states of the AO in the path state $|1\rangle$, respectively. Then, the state transformation of the photon corresponding to the AO state is given as follows.

- $AO = |0\rangle_{AO}$: In the absence of the AO, the split components of the photon in path states $|0\rangle$ and $|1\rangle$ recombine at $BS_2^{(\pi/4)}$ and transform as

$$|\psi_2\rangle = \frac{1}{2} (|0\rangle + |1\rangle - |0\rangle + |1\rangle) = |1\rangle. \quad (13)$$

This is due to the destructive interference and D_0 clicks with certainty.

- $AO = |1\rangle_{AO}$: In the presence of the AO, if the photon is absorbed by the AO, no photon reaches to $BS_2^{(\pi/4)}$. Unless it is absorbed, due to the constructive interference after $BS_2^{(\pi/4)}$, the detectors D_0 and D_1 click with equal probability. Since D_0 can click in both the absence state $|0\rangle_{AO}$ and the presence state $|1\rangle_{AO}$, it gives no certain information about the AO existence. In case D_1 clicks, it is inferred that the AO is present in the interferometer, while the photon has not interacted with the AO. Note that if the photon is not absorbed by the AO, it was not in the path state $|1\rangle$ at any stage of the protocol, which forms the basis of counterfactual quantum protocols.

In the presence of the AO, the photon after $BS_1^{(\pi/4)}$ is in an unstable quantum state—either absorbed by the AO or arrive at $BS_2^{(\pi/4)}$. The efficiency of the EV-IFM is limited by the margin of 50% due to the very low frequency of measurements performed on the unstable quantum state of the photon and the balanced beam splitters.²

2) *KW-IFM*: As the measurement (AO presence) is performed only once in the EV-IFM, the decay rate of the photon (unstable quantum state) is $1/2$ [83]. To reduce the decay rate arbitrarily close to zero, the QZ IFM has been proposed to perform repeated measurements on the unstable quantum state of the photon [30]. Fig. 3 shows in principle the decay rate for this IFM approaches zero under the asymptotic limits with N unbalanced beam splitters $BS_i^{(\theta_N)}$, $i = 1, 2, \dots, N$, where $\theta_N = \pi/(2N)$. To determine the AO existence in the path state $|1\rangle$, assume that the initial state of the photon is $|\psi_0\rangle = |0\rangle$. As illustrated in Fig. 3, when the photon reaches $BS_1^{(\theta_N)}$, it creates the unbalanced spatial superposition under the unitary operation $R_y(2\theta_N)$ as follows:

$$\begin{aligned} |\psi_1\rangle &= R_y(2\theta_N) |\psi_0\rangle \\ &= \cos \theta_N |0\rangle + \sin \theta_N |1\rangle. \end{aligned} \quad (14)$$

The state transformation of the photon corresponding to the AO state is given as follows.

- $AO = |0\rangle_{AO}$: In the absence of the AO, each beam splitter gives the rotation of angle θ_N . After the i th beam splitter $BS_i^{(\theta_N)}$, the photon state is given by

$$|\psi_i\rangle = \cos(i\theta_N) |0\rangle + \sin(i\theta_N) |1\rangle. \quad (15)$$

At the end of the protocol, the photon state transforms as $|\psi_N\rangle = R_y^N(2\theta_N) |\psi_0\rangle = |1\rangle$ and the detector D_0 clicks with certainty.

²The AO presence is similar to performing a measurement on the photon in computational basis.

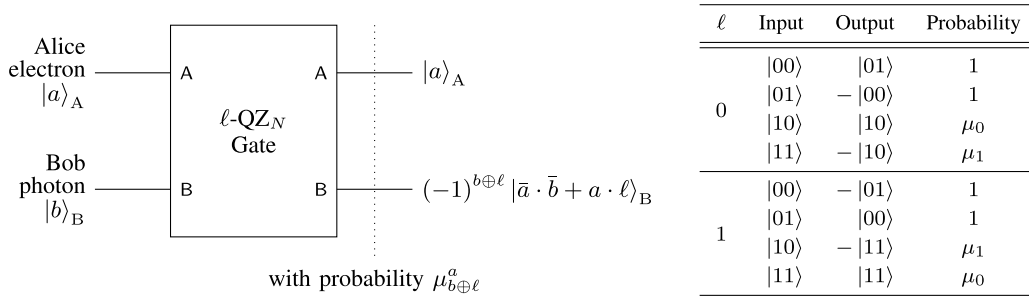


Fig. 4. An ℓ -QZ $_N$ gate where $|ab\rangle_{AB} \rightarrow (-1)^{b \oplus \ell} |a(\bar{a} \cdot \bar{b} + a \cdot \ell)\rangle_{AB}$ with the probability $\mu_{b \oplus \ell}^a$.

- AO = $|1\rangle_{AO}$: In the presence of the AO, there is a nonzero probability that the photon is absorbed by the AO in each cycle. Unless it is absorbed, after the i th beam splitter BS $_i^{(\theta_N)}$, the photon state is given by

$$|\psi_i\rangle = \cos^i \theta_N |0\rangle + \sin \theta_N \cos^{i-1} \theta_N |1\rangle. \quad (16)$$

Since the photon component in the path state $|1\rangle$ only interacts with the AO, the probability that the photon is absorbed by the AO in the i th cycle is

$$q_i = \sin^2 \theta_N \cos^{2(i-1)} \theta_N. \quad (17)$$

At the end of the protocol, the photon state collapses back to the initial state and the detector D $_1$ clicks with the probability

$$\mu_0 = \cos^{2N} \theta_N. \quad (18)$$

Unless the protocol is discarded in the KW-IFM, we can ascertain the absence or presence of the AO in the interferometer with certainty since only D $_a$ clicks for AO = $|a\rangle_{AO}$, $a \in \mathbb{Z}_2$. As $N \rightarrow \infty$, the probability μ_0 tends to one (the absorption probability $q_i \rightarrow 0$), demonstrating the QZ effect.

D. QZ Gates

The QZ gates are the Michelson version of the KW-IFM to ascertain the existence of a classical AO in the interferometer by using two (i.e., polarization and path) degrees of freedom in the photon with the combination of a switchable mirror (SM), a polarization rotator (PR), a polarizing beam splitter (PBS), an optical delay (OD), and optical circulators (OCs) [31], [41]. Let $|a\rangle_A = |a\rangle_{AO}$ be the AO state of Alice and

$$\begin{aligned} |0\rangle_B &= |H\rangle_p \\ |1\rangle_B &= |V\rangle_p \end{aligned} \quad (19)$$

be horizontally and vertically polarized photons of Bob, where the subscripts p, A, and B denote the photon polarization, Alice, and Bob, respectively. The ℓ -QZ $_N$ gate with N cycles takes Bob's $|b\rangle_B$ polarized photon as input and Alice's classical AO $|a\rangle_A$ as control where $b, \ell \in \mathbb{Z}_2$ (see [41, Fig. 1]). When $b = \ell$, this gate infers the absence $|0\rangle_A$ of Alice's AO by Bob's output $|\bar{b}\rangle_B$ or the presence $|1\rangle_A$ by the output $|b\rangle_B$ —in particular counterfactually for $|1\rangle_A$ (see [41, Sec. 2.1]).³ As shown in Fig. 4, the overall action of the QZ gate is

³For binary variables $a, b \in \mathbb{Z}_2$, we denote the bitwise OR, AND, XOR, and NOT (bit flip) operations by $a + b$, $a \cdot b$, $a \oplus b$, and \bar{b} , respectively.

generally as follows:

$$\ell\text{-QZ}_N : \begin{cases} |ab\rangle_{AB} \rightarrow (-1)^{b \oplus \ell} |a(\bar{a} \cdot \bar{b} + a \cdot \ell)\rangle_{AB} \\ \text{with the probability } \mu_{b \oplus \ell}^a, \end{cases} \quad (20)$$

where

$$\mu_1 = \sin^2 \theta_N (1 - \sin^2 \theta_N)^{N-1}. \quad (21)$$

Heretofore, we consider only the classical behavior of the AO and the photon for QZ gates. In general, the quantum AO (QAO) can be in the superposition of absence and presence states such as an electron in the superposition state of the up spin $|\uparrow\rangle_e$ and down spin $|\downarrow\rangle_e$ (see [41, Fig. 6(b)]). Since μ_1 tends to zero as $N \rightarrow \infty$, we now consider a general composite state of Alice's QAO and Bob's photon for the ℓ -QZ $_N$ gate as follows:

$$|qz_\ell\rangle_{AB} = x|00\rangle_{AB} + y|01\rangle_{AB} + z|1\ell\rangle_{AB}, \quad (22)$$

where x, y , and z are complex coefficients with $|x|^2 + |y|^2 + |z|^2 = 1$ and

$$\begin{aligned} |0\rangle_A &= |\uparrow\rangle_e \\ |1\rangle_A &= |\downarrow\rangle_e. \end{aligned} \quad (23)$$

Unless the photon is absorbed, the ℓ -QZ $_N$ gate transforms the input state $|qz_\ell\rangle_{AB}$ as follows:

$$\begin{aligned} \ell\text{-QZ}_N(|qz_\ell\rangle_{AB}) &= (-1)^\ell x|01\rangle_{AB} \\ &\quad + (-1)^{\bar{\ell}} y|00\rangle_{AB} + z|1\ell\rangle_{AB} \end{aligned} \quad (24)$$

with the probability

$$\lambda_1 = (1 - |z|^2 \sin^2 \theta_N)^N \quad (25)$$

tending to one as $N \rightarrow \infty$. From (24), the QZ $_N$ gate for the input state $|qz_\ell\rangle_{AB}$ is configured as non-unitary transformation such that

$$\ell\text{-QZ}_N : \begin{cases} (-1)^{b \oplus \ell} (|0\rangle_A \langle 0| \otimes \mathbf{X} + |1\rangle_A \langle 1| \otimes |\ell\rangle_B \langle \ell|) \\ \text{with the probability } \lambda_1. \end{cases} \quad (26)$$

E. CQZ and D-CQZ Gates

1) *CQZ Gates*: The CQZ gates are the nested version of the QZ gates to counterfactually ascertain both the absence and presence of a classical AO in the interferometer [24], [33], [41]. Taking again Bob's photon $|b\rangle_B$ as input and Alice's AO $|a\rangle_A$ as control (see [41, Fig. 2]), the ℓ -CQZ $_{M,N}$ gate with

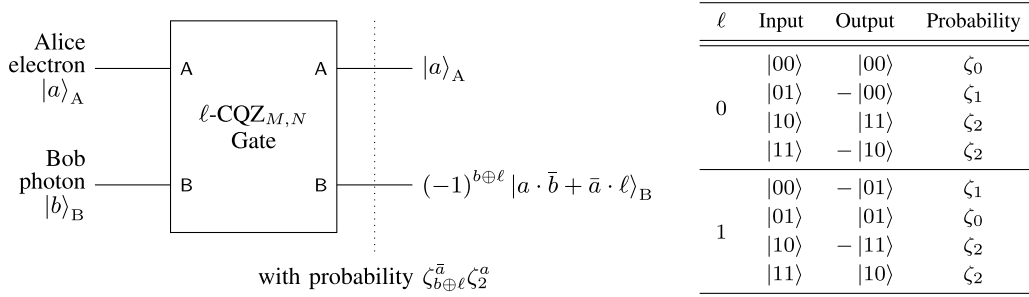


Fig. 5. An ℓ -CQZ $_{M,N}$ gate where $|ab\rangle_{AB} \rightarrow (-1)^{b\oplus\ell} |a \cdot \bar{b} + \bar{a} \cdot \ell\rangle_{AB}$ with the probability $\zeta_{b\oplus\ell}^{\bar{a}} \zeta_2^a$.

M outer and N inner cycles determines the absence $|0\rangle_A$ of Alice's AO by Bob's output $|b\rangle_B$ or the presence $|1\rangle_A$ by the output $|\bar{b}\rangle_B$ in both counterfactually when $b = \ell$ (see [41, Sec. 2.2]). As shown in Fig. 5, the overall map of the CQZ gate is generally as follows:

$$\ell\text{-CQZ}_{M,N} : \begin{cases} |ab\rangle_{AB} \rightarrow (-1)^{b\oplus\ell} |a \cdot \bar{b} + \bar{a} \cdot \ell\rangle_{AB} \\ \text{with the probability } \zeta_{b\oplus\ell}^{\bar{a}} \zeta_2^a, \end{cases} \quad (27)$$

where

$$\zeta_0 = f(1, 0), \quad (28)$$

$$\zeta_1 = \sin^2 \theta_M (1 - \sin^2 \theta_M)^{M-1}, \quad (29)$$

$$\zeta_2 = f(0, 1), \quad (30)$$

and with $u, v \in [0, 1]$

$$f(u, v) = (1 - u \sin^2 \theta_M)^M \times \prod_{i=1}^M [1 - v \sin^2(i\theta_M) \sin^2 \theta_N]^N \quad (31)$$

tending to one as $M, N \rightarrow \infty$. Since ζ_1 goes to zero as $M \rightarrow \infty$, we also consider a general composite state of Alice and Bob for the ℓ -CQZ $_{M,N}$ gate as follows:

$$|cqz_\ell\rangle_{AB} = x|0\ell\rangle_{AB} + y|10\rangle_{AB} + z|11\rangle_{AB}. \quad (32)$$

Unless the photon is absorbed, the ℓ -CQZ $_{M,N}$ gate transforms the input state $|cqz_\ell\rangle_{AB}$ as follows:

$$\begin{aligned} \ell\text{-CQZ}_{M,N}(|cqz_\ell\rangle_{AB}) \\ = x|0\ell\rangle_{AB} + (-1)^\ell y|11\rangle_{AB} + (-1)^{\bar{\ell}} z|10\rangle_{AB} \end{aligned} \quad (33)$$

with the probability

$$\lambda_2 = f(|x|^2, |y|^2 + |z|^2) \quad (34)$$

tending to one as $M, N \rightarrow \infty$. From (33), the CQZ $_{M,N}$ gate for the input state $|cqz_\ell\rangle_{AB}$ is configured as non-unitary transformation such that

$$\ell\text{-CQZ}_{M,N} : \begin{cases} (-1)^{b\oplus\ell} (|0\rangle_A \langle 0| \otimes |\ell\rangle_B \langle \ell| + |1\rangle_A \langle 1| \otimes \mathbf{X}) \\ \text{with the probability } \lambda_2. \end{cases} \quad (35)$$

2) *D-CQZ Gates*: The D-CQZ gate is the dual form of CQZ gates where Bob's ancilla qubit C carries the path information of the photon (see [41, Fig. 12]). The D-CQZ $_{M,N}$ gate with M outer and N inner cycles takes Bob's $|b\rangle_B$ polarized photon in the path state $|c\rangle_C$ as input and Alice's AO $|a\rangle_A$ as control where $c \in \mathbb{Z}_2$. As shown in Fig. 6, the overall operation of the D-CQZ gate is generally as follows:

$$\text{D-CQZ}_{M,N} : \begin{cases} |abc\rangle_{ABC} \rightarrow (-1)^{b\oplus c} |a \cdot \bar{b} + \bar{a} \cdot c\rangle_{ABC} \\ \text{with the probability } \zeta_{b\oplus c}^{\bar{a}} \zeta_2^a. \end{cases} \quad (36)$$

Unless the photon is absorbed, the D-CQZ $_{M,N}$ gate transforms the general input state

$$|dcqz\rangle_{ABC} = \gamma |cqz_0\rangle_{AB} |0\rangle_C + \delta |cqz_1\rangle_{AB} |1\rangle_C \quad (37)$$

as follows:

$$\begin{aligned} \text{D-CQZ}_{M,N}(|dcqz\rangle_{ABC}) \\ = \gamma x |000\rangle_{ABC} + \gamma y |110\rangle_{ABC} - \gamma z |100\rangle_{ABC} \\ + \delta x |011\rangle_{ABC} - \delta y |111\rangle_{ABC} + \delta z |101\rangle_{ABC} \end{aligned} \quad (38)$$

with the probability λ_2 where $|\gamma|^2 + |\delta|^2 = 1$.

F. MQZ and D-MQZ Gates

1) *MQZ Gates*: The MQZ gate is the modified form of the QZ gate where its main advantage is obtained from the quantum behavior of the AO (see [41, Fig. 7]). Taking Bob's photon $|b\rangle_B$ as input and Alice's AO $|a\rangle_A$ as control, the overall operation of the ℓ -MQZ $_N$ gate with N cycles is generally as follows (see Fig. 7):

$$\ell\text{-MQZ}_N : \begin{cases} |ab\rangle_{AB} \rightarrow (-1)^{b\oplus\ell} |a\ell\rangle_{AB} \\ \text{with the probability } \mu_{b\oplus\ell}^{\bar{a}} \Delta_{a,b,\ell}, \end{cases} \quad (39)$$

where $\Delta_{a,b,\ell} = 0$ if $a \neq b = \ell$, otherwise $\Delta_{a,b,\ell} = 1$. Since the photon is absorbed by the electron with certainty for $a \neq b = \ell$ (i.e., $\Delta_{a,b,\ell} = 0$) and μ_1 approaches zero as $N \rightarrow \infty$, we consider a composite input state of Alice and Bob for the ℓ -MQZ $_N$ gate as follows:

$$|mqz_\ell\rangle_{AB} = (\alpha_0 |0\rangle_A + \alpha_1 |1\rangle_A) |\ell\rangle_B, \quad (40)$$

where $|\alpha_0|^2 + |\alpha_1|^2 = 1$. Unless the photon is absorbed by the electron, the ℓ -MQZ $_N$ gate transforms the input state $|mqz_\ell\rangle_{AB}$ as follows:

$$\ell\text{-MQZ}_N(|mqz_\ell\rangle_{AB}) = |\ell\ell\rangle_{AB} \quad (41)$$

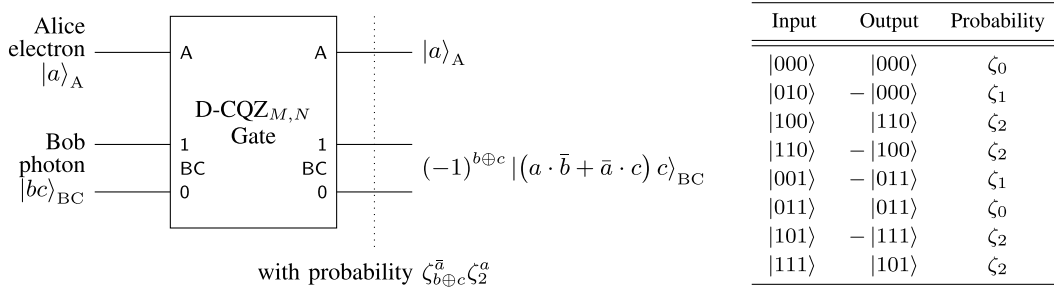


Fig. 6. A D-CQZ_{M,N} gate where $|abc\rangle_{ABC} \rightarrow (-1)^{b\oplus c} |(a \cdot \bar{b} + \bar{a} \cdot c) c\rangle_{ABC}$ with the probability $\zeta_{b\oplus c}^{\bar{a}} \zeta_2^a$.

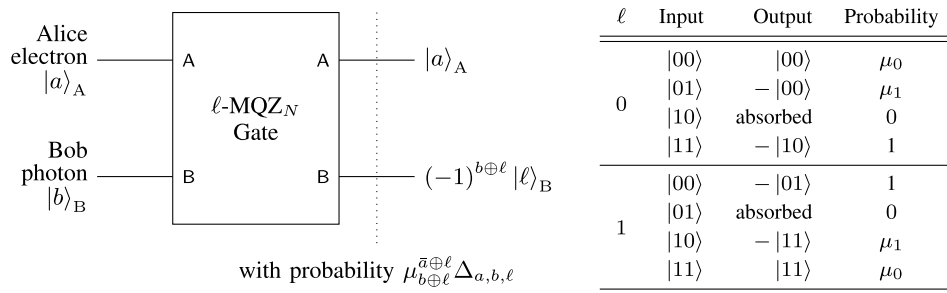


Fig. 7. An ℓ -MQZ_N gate where $|ab\rangle_{AB} \rightarrow (-1)^{b\oplus \ell} |a\ell\rangle_{AB}$ with the probability $\mu_{b\oplus \ell}^{\bar{a}\oplus \ell} \Delta_{a,b,\ell}$.

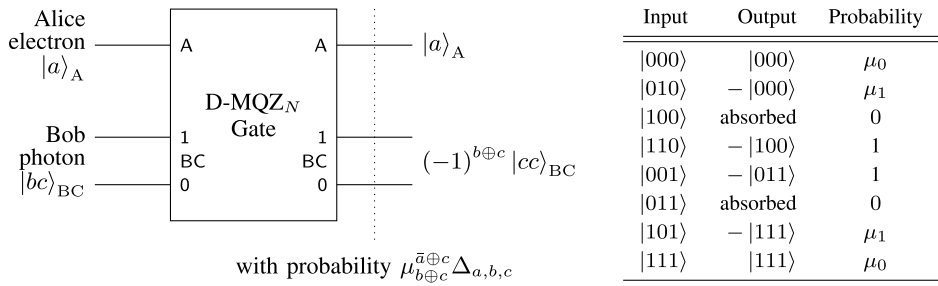


Fig. 8. A D-MQZ_N gate where $|abc\rangle_{ABC} \rightarrow (-1)^{b\oplus c} |acc\rangle_{ABC}$ with the probability $\mu_{b\oplus c}^{\bar{a}\oplus c} \Delta_{a,b,c}$.

with the probability $\lambda_3 = h(|\alpha_\ell|^2)$ where

$$h(x) = x(1 - x \sin^2 \theta_N)^N. \quad (42)$$

2) *D-MQZ Gates*: Similar to D-CQZ gates, the D-MQZ gate is the dual form of MQZ gates (see [41, Fig. 11]). The D-MQZ_N gate with N cycles takes Bob's $|b\rangle_B$ polarized photon in the path state $|c\rangle_C$ as input and Alice's AO $|a\rangle_A$ as control. As shown in Fig. 8, the overall operation of the D-MQZ gate is generally as follows:

$$\text{D-MQZ}_N : \begin{cases} |abc\rangle_{ABC} \rightarrow (-1)^{b\oplus c} |acc\rangle_{ABC} \\ \text{with the probability } \mu_{b\oplus c}^{\bar{a}\oplus c} \Delta_{a,b,c}. \end{cases} \quad (43)$$

Unless the photon is absorbed, the D-MQZ_N gate transforms the general input state

$$|\text{dmqz}\rangle_{ABC} = \gamma |\text{mqz}_0\rangle_{AB} |0\rangle_C + \delta |\text{mqz}_1\rangle_{AB} |1\rangle_C \quad (44)$$

as follows:

$$\text{D-MQZ}_N (|\text{dmqz}\rangle_{ABC}) = \gamma |000\rangle_{ABC} + \delta |111\rangle_{ABC} \quad (45)$$

with the probability $\lambda_4 = h(|\gamma\alpha_0|^2 + |\delta\alpha_1|^2)$.

G. DCF Gates

To devise the ℓ -DCF_{K,N} gate, K ℓ -MQZ_N gates are concatenated serially (see Fig. 9). Taking Bob's photon $|b\rangle_B$ as control and Alice's AO $|a\rangle_A$ as a target, the controlled flipping operation of the ℓ -DCF_{K,N} gate is generally as follows:

$$\ell\text{-DCF}_{K,N} : \begin{cases} |ab\rangle_{AB} \rightarrow (-1)^{a+b+\ell} |(a \oplus b) b\rangle_{AB} \\ \text{with the probability } \zeta_3^{\bar{b}} \Delta_{a,b\oplus \ell, \ell}, \end{cases} \quad (46)$$

where $\zeta_3 = g(1)$ and

$$g(u) = (1 - u \sin^2 \theta_K)^K \times (1 - u \cos^2 \theta_K \sin^2 \theta_N)^{KN} \quad (47)$$

tending to one as $K, N \rightarrow \infty$. Since the photon is absorbed by the electron with certainty when $b = 0$ and $a \neq \ell$ (i.e., $\Delta_{a,b\oplus \ell, \ell} = 0$), we consider a general composite input state of Alice and Bob for the ℓ -DCF_{K,N} gate as follows:

$$|\text{dcf}_\ell\rangle_{AB} = x |\ell 0\rangle_{AB} + y |0 1\rangle_{AB} + z |1 1\rangle_{AB}. \quad (48)$$

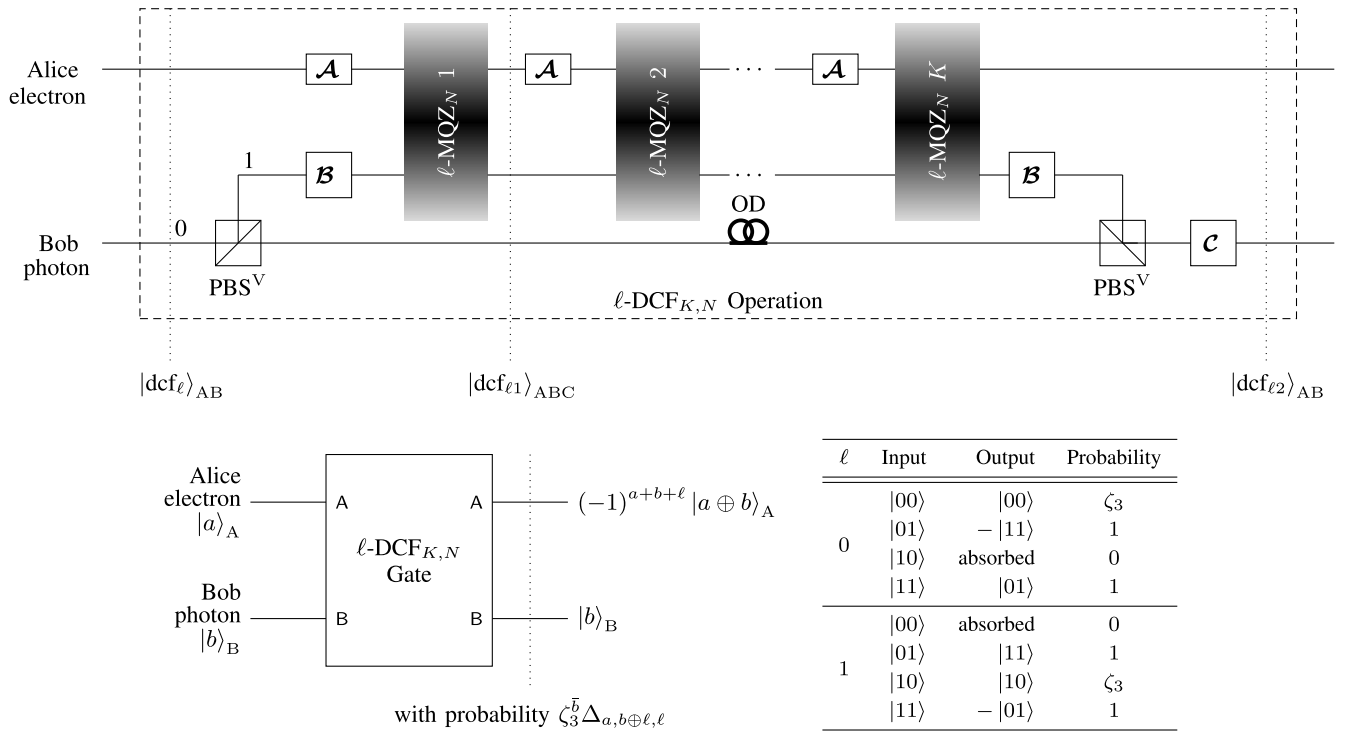


Fig. 9. An ℓ -DCF $_{K,N}$ gate where $|ab\rangle_{AB} \rightarrow (-1)^{a+b+\ell} |(a \oplus b)b\rangle_{AB}$ with the probability $\zeta_3^b \Delta_{a,b \oplus \ell, \ell}$. Here, $\mathcal{A} = R_y(2\theta_K)$, $\mathcal{B} = X^\ell$, $\mathcal{C} = Z^\ell$, and K is the number of ℓ -MQZ $_N$ gates.

- 1) Bob starts the ℓ -DCF $_{K,N}$ protocol by applying PBS V on his photon, which allows the vertical photon component $|1\rangle_B$ to pass in the path state $|0\rangle_C$ and detour the horizontal component $|0\rangle_B$ in the path state $|1\rangle_C$ to be recombined after K successive ℓ -MQZ $_N$ operations. Bob performs the \mathcal{B} operator on his photon $|0\rangle_B$ in the path state $|1\rangle_C$ to ensure the input $|\ell\rangle_B$ for the ℓ -MQZ $_N$ gate where $\mathcal{B} = X^\ell$.
- 2) Alice performs the \mathcal{A} operator on her qubit (electron) where $\mathcal{A} = R_y(2\theta_K)$. The rotation gate \mathcal{A} transforms $|a\rangle_A$ as follows:

$$\mathcal{A}|a\rangle_A = \cos \theta_K |a\rangle_A + (-1)^a \sin \theta_K |\bar{a}\rangle_A. \quad (49)$$

- 3) Alice and Bob input her qubit and his photon component $|\ell\rangle_B$ in the path state $|1\rangle_C$ to the ℓ -MQZ $_N$ gate, respectively. Unless the photon is absorbed by the electron, the first ℓ -MQZ $_N$ gate transforms the state $|\text{dcf}_\ell\rangle_{AB}$ as follows:

$$\begin{aligned} |\text{dcf}_\ell\rangle_{ABC} &= x |\ell\ell\rangle_{ABC} \\ &+ \cos \theta_K (y |0\rangle_A + z |1\rangle_A) |10\rangle_{BC} \\ &+ \sin \theta_K (y |1\rangle_A - z |0\rangle_A) |10\rangle_{BC}. \end{aligned} \quad (50)$$

Whenever the photon is found in the quantum channel between Alice and Bob, the electron absorbs it and the protocol declares an erasure.

- 4) Alice and Bob repeat the second and third steps for subsequent ℓ -MQZ $_N$ gates. After K ℓ -MQZ $_N$ gates, unless the photon is absorbed by the electron, Bob performs the \mathcal{B} operator again on the photon component in the path state $|1\rangle_C$ to recombine the horizontal and

vertical components of the photon by PBS V . At the end of the protocol, Bob performs the \mathcal{C} operator on his qubit to complete the ℓ -DCF $_{K,N}$ protocol where $\mathcal{C} = Z^\ell$. Then, the composite state of Alice and Bob transforms as follows:

$$\begin{aligned} |\text{dcf}_{\ell 2}\rangle_{AB} &= x |\ell 0\rangle_{AB} + (-1)^{\bar{\ell}} y |11\rangle_{AB} \\ &+ (-1)^\ell z |01\rangle_{AB} \end{aligned} \quad (51)$$

with the probability $\lambda_5 = g(|x|^2)$.

Unless the protocol is discarded, the DCF $_{K,N}$ gate for the input state $|\text{dcf}_\ell\rangle_{AB}$ is configured as the controlled flipping operation in (51) such that

$$\ell\text{-DCF}_{K,N} : \begin{cases} \mathbf{I} \otimes |0\rangle_B \langle 0| + (-1)^{\bar{\ell}} \mathbf{X} \mathbf{Z} \otimes |1\rangle_B \langle 1| \\ \text{with the probability } \lambda_5, \end{cases} \quad (52)$$

where the polarization state of Bob's photon acts as a control qubit and the QAO state of Alice's electron acts as a target qubit.

H. D-DCF Gates

Similar to the ℓ -DCF $_{K,N}$ operation, K D-MQZ $_N$ gates are concatenated serially to devise the D-DCF $_{K,M}$ gate, as shown in Fig. 10. Taking Bob's $|b\rangle_B$ polarized photon in the path state $|c\rangle_C$ as control and Alice's AO $|a\rangle_A$ as a target, the controlled flipping operation of the D-DCF $_{K,N}$ gate is generally as follows:

$$\text{D-DCF}_{K,N} : \begin{cases} |abc\rangle_{ABC} \rightarrow (-1)^{a+b+c} |(a \oplus b)bc\rangle_{ABC} \\ \text{with the probability } \zeta_3^{\bar{b}} \Delta_{a,b \oplus c, c}. \end{cases} \quad (53)$$

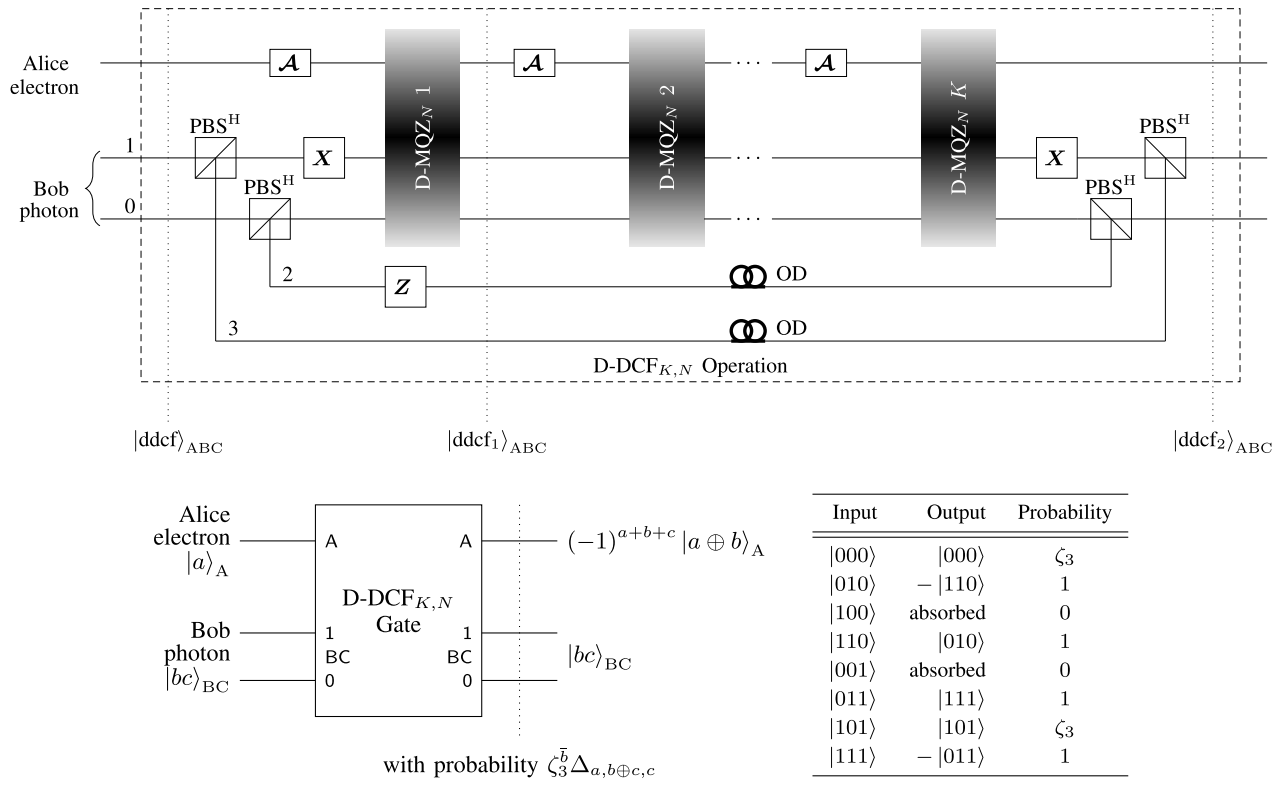


Fig. 10. A D-DCF $_{K,N}$ gate where $|abc\rangle_{ABC} \rightarrow (-1)^{a+b+c} |(a \oplus b)bc\rangle_{ABC}$ with the probability $\zeta_3^b \Delta_{a,b \oplus c,c}$.

Since the photon is absorbed by the electron with certainty when $b = 0$ and $a \neq c$ (i.e., $\Delta_{a,b \oplus c,c} = 0$), we consider a composite input state of Alice and Bob for the D-DCF $_{K,N}$ gate as follows:

$$|\text{ddcf}\rangle_{ABC} = \gamma |\text{dcf}_0\rangle_{AB} |0\rangle_C + \delta |\text{dcf}_1\rangle_{AB} |1\rangle_C. \quad (54)$$

- 1) Bob starts the D-DCF $_{K,N}$ protocol by applying PBS^H in each path of the photon and recombines the respective photon components after K successive D-MQZ $_N$ operations. Bob performs the X and Z operators on his photon components in path states $|1\rangle_C$ and $|2\rangle_C$, respectively.
- 2) Alice performs $\mathcal{A} = R_y(2\theta_K)$ on her qubit and Bob inputs his photon components in path states $|0\rangle_C$ and $|1\rangle_C$ to the D-MQZ $_N$ gate, respectively. Unless the photon is absorbed by the electron, the first D-MQZ $_N$ gate transforms the input state $|\text{ddcf}\rangle_{ABC}$ to

$$\begin{aligned} |\text{ddcf}_1\rangle_{ABC} &= \gamma x |000\rangle_{ABC} + \delta x |111\rangle_{ABC} \\ &\quad - \gamma \cos \theta_K (y |0\rangle_A + z |1\rangle_A) |12\rangle_{BC} \\ &\quad - \gamma \sin \theta_K (y |1\rangle_A - z |0\rangle_A) |12\rangle_{BC} \\ &\quad + \delta \cos \theta_K (y |0\rangle_A + z |1\rangle_A) |13\rangle_{BC} \\ &\quad + \delta \sin \theta_K (y |1\rangle_A - z |0\rangle_A) |13\rangle_{BC}. \end{aligned} \quad (55)$$

- 3) Alice and Bob repeat the second step for the subsequent D-MQZ $_N$ gates. After K D-MQZ $_N$ gates, unless the photon is absorbed, Bob performs the X operator on his photon component in the path state $|1\rangle_C$ and recombines the respective photon components. The composite state

of Alice and Bob transforms as follows:

$$\begin{aligned} |\text{ddcf}_2\rangle_{ABC} &= \gamma |\text{dcf}_02\rangle_{AB} |0\rangle_C + \delta |\text{dcf}_12\rangle_{AB} |1\rangle_C \\ &= \gamma x |000\rangle_{ABC} - \gamma y |110\rangle_{ABC} + \gamma z |010\rangle_{ABC} \\ &\quad + \delta x |101\rangle_{ABC} + \delta y |111\rangle_{ABC} - \delta z |011\rangle_{ABC} \end{aligned} \quad (56)$$

with the probability λ_5 .

Unless the protocol is discarded, the D-DCF $_{K,N}$ gate for the input state $|\text{ddcf}\rangle_{ABC}$ is configured as the controlled flipping operation in (56) such that

$$\text{D-DCF}_{K,N} : \begin{cases} Z \otimes |0\rangle_B \langle 0| \otimes Z - XZ \otimes |1\rangle_B \langle 1| \otimes Z \\ \text{with the probability } \lambda_5, \end{cases} \quad (57)$$

where the polarization state of Bob's photon acts as a control qubit and the QAO state of Alice's electron acts as a target qubit.

IV. QUANTUM TELECOMPUTATION

In this section, we propose two quantum teleportation protocols: a *stochastic* CCT protocol for general input states and a *deterministic* CCT protocol for Bell-type input states. These counterfactual protocols allow Bob to perform an arbitrary single-qubit unitary operation on Alice's qubit in a concealed, controlled, and counterfactual manner.

A. CCT Protocols

Let U be the single-qubit unitary operator in (4) and

$$U_m = R_z(\phi) R_y(\theta; m) R_z(\varphi) \quad (58)$$

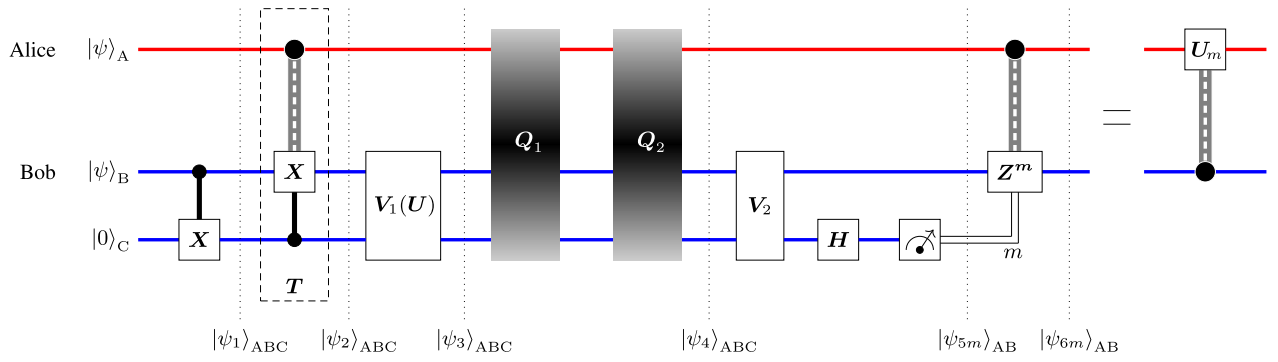


Fig. 11. A stochastic CCT protocol without preshared entanglement. Bob starts the protocol by entangling his qubit $|\psi\rangle_B$ and ancilla $|0\rangle_C$ with the local CNOT operation. Alice and Bob apply a sequence of nonlocal controlled flipping operations T , Q_1 , Q_2 and the local operations $V_1(U)$, V_2 (at Bob's side). At the end of the protocol, Bob applies the Hadamard gate H on the ancilla followed by measuring the ancilla in the computational basis. Alice and Bob counterfactually apply the controlled- Z^m operation on their composite state and transform it as $|\psi_{6m}\rangle_{AB} = \gamma |\psi\rangle_A |0\rangle_B + \delta (U_m |\psi\rangle_A) |1\rangle_B$ where $U_m = R_z(\phi) R_y(\theta; m) R_z(\varphi)$.

denote its pair for two directions of y -rotation where $m \in \mathbb{Z}_2$. The CCT protocol counterfactually performs the controlled- U_m operation on Alice's qubit with

$$\Pr[m = m] = \begin{cases} \frac{1}{2}, & \text{for } m = 0, \\ \frac{1}{2}, & \text{for } m = 1 \end{cases} \quad (59)$$

without revealing U_m to Alice as shown in Fig. 11. To demonstrate the implementation of CCT, we consider arbitrary pure input states of Alice's target qubit $|\psi\rangle_A$ and Bob's control qubit $|\psi\rangle_B$ as follows:

$$|\psi\rangle_A = \alpha |0\rangle_A + \beta |1\rangle_A, \quad (60)$$

$$|\psi\rangle_B = \gamma |0\rangle_B + \delta |1\rangle_B. \quad (61)$$

Bob starts the protocol by performing the local CNOT operation to entangle his qubit with the ancillary qubit $|0\rangle_C$. Then, Alice and Bob have the separable composite state $|\psi_1\rangle_{ABC}$ as follows:

$$|\psi_1\rangle_{ABC} = |\psi\rangle_A (\gamma |00\rangle_{BC} + \delta |11\rangle_{BC}). \quad (62)$$

Alice and Bob counterfactually apply the Toffoli gate T with Alice's qubit and Bob's ancillary qubit as control and Bob's qubit as a target. To ensure the counterfactuality of the protocol, if any physical particle is transmitted over the quantum channel, Alice's QAO absorbs the particle and both parties (Alice and Bob) discard the protocol. Unless the protocol is discarded, it transforms the composite state $|\psi_1\rangle_{ABC}$ as follows:

$$|\psi_2\rangle_{ABC} = \gamma |\psi\rangle_A |00\rangle_{BC} + \delta (\alpha |01\rangle_{AB} + \beta |10\rangle_{AB}) |1\rangle_C. \quad (63)$$

Bob applies the following local operation $V_1(U)$ on his qubit and ancillary qubit:

$$V_1(U) = V_{14} V_{13} V_{12} V_{11}, \quad (64)$$

where

$$V_{11} = I \otimes |0\rangle_C \langle 0| + (R_z(\varphi) X) \otimes |1\rangle_C \langle 1|, \\ + I \otimes |2\rangle_C \langle 2|, \quad (65)$$

$$V_{12} = |0\rangle_B \langle 0| \otimes I + |10\rangle_{BC} \langle 10| + |12\rangle_{BC} \langle 11| \\ + |11\rangle_{BC} \langle 12|, \quad (66)$$

$$V_{13} = I \otimes |0\rangle_C \langle 0| + (R_z(\phi) R_y(\theta)) \otimes |1\rangle_C \langle 1| \\ + (R_z(\phi) R_y(\theta)) \otimes |2\rangle_C \langle 2|, \quad (67)$$

$$V_{14} = I \otimes (|0\rangle_C \langle 0| + |2\rangle_C \langle 2|) + X \otimes |1\rangle_C \langle 1|. \quad (68)$$

Note that the dependence of V_1 on U is through V_{11} and V_{13} . As a controlled manner, this operation encodes U on Bob's qubit as follows:

$$V_1 |01\rangle_{BC} = (UX |0\rangle_B) |2\rangle_C, \quad (69)$$

$$V_1 |11\rangle_{BC} = (XUX |1\rangle_B) |1\rangle_C. \quad (70)$$

Since

$$U |b\rangle_B = e^{(-1)^b \varphi(\varphi+\phi)/2} \cos(\theta/2) |b\rangle_B \\ + (-1)^b e^{(-1)^b \varphi(\varphi-\phi)/2} \sin(\theta/2) |\bar{b}\rangle_B, \quad (71)$$

it transforms the composite state $|\psi_2\rangle_{ABC}$ as follows:

$$|\psi_3\rangle_{ABC} = \gamma |\psi\rangle_A |00\rangle_{BC} \\ + \delta \alpha e^{-i(\varphi+\phi)/2} \cos(\theta/2) |011\rangle_{ABC} \\ + \delta \alpha e^{-i(\varphi-\phi)/2} \sin(\theta/2) |001\rangle_{ABC} \\ + \delta \beta e^{i(\varphi+\phi)/2} \cos(\theta/2) |112\rangle_{ABC} \\ - \delta \beta e^{i(\varphi-\phi)/2} \sin(\theta/2) |102\rangle_{ABC}. \quad (72)$$

Now, Alice and Bob counterfactually apply the following consecutive controlled flipping operations Q_1 and Q_2 where

$$Q_1 = I \otimes (|00\rangle_{BC} \langle 00| + |10\rangle_{BC} \langle 10| \\ + |11\rangle_{BC} \langle 11| - |12\rangle_{BC} \langle 12|) \\ + X \otimes (|02\rangle_{BC} \langle 02| - |01\rangle_{BC} \langle 01|), \quad (73)$$

$$Q_2 = |0\rangle_A \langle 0| \otimes I \otimes (|0\rangle_C \langle 0| + |1\rangle_C \langle 1|) \\ + |1\rangle_A \langle 1| \otimes I \otimes (|0\rangle_C \langle 0| - |2\rangle_C \langle 2|) \\ - |1\rangle_A \langle 1| \otimes X \otimes |1\rangle_C \langle 1| \\ + |0\rangle_A \langle 0| \otimes X \otimes |2\rangle_C \langle 2|. \quad (74)$$

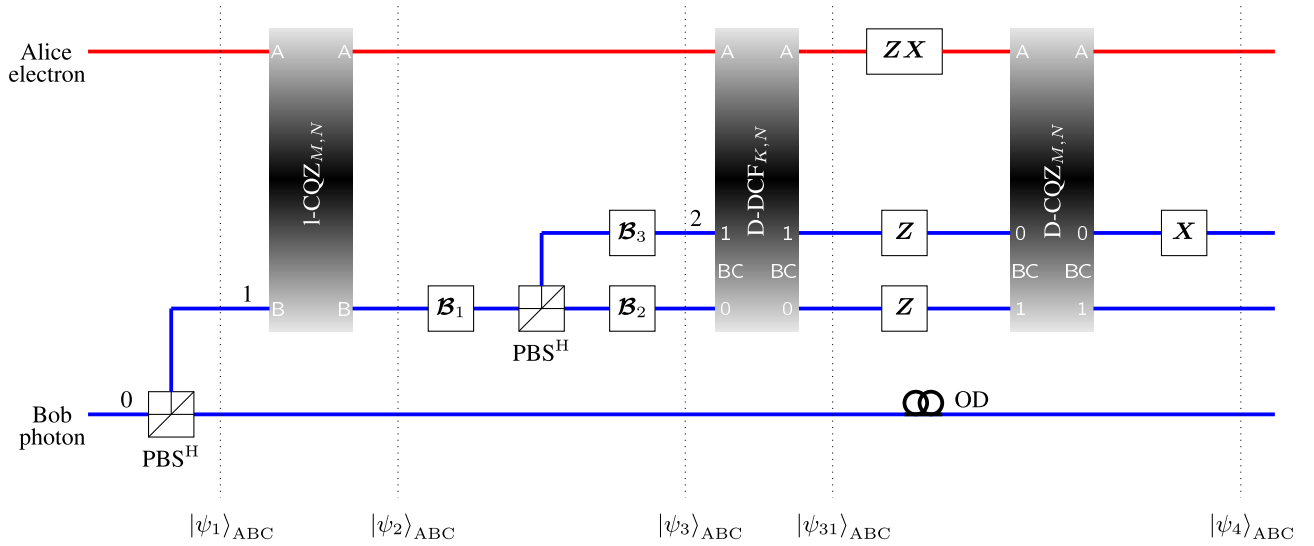


Fig. 12. A CCT protocol for general input states using QZ and CQZ gates. Here $\mathbf{B}_1 = \mathbf{R}_z(\varphi) \mathbf{X}$, $\mathbf{B}_2 = \mathbf{R}_z(\phi) \mathbf{R}_y(\theta)$, and $\mathbf{B}_3 = \mathbf{X} \mathbf{B}_2$.

Unless the protocol is discarded, the global controlled flipping operations transform the composite state $|\psi_3\rangle_{ABC}$ as follows:

$$\begin{aligned} |\psi_4\rangle_{ABC} = & \gamma |\psi\rangle_A |00\rangle_{BC} \\ & + \delta \alpha e^{-i(\varphi+\phi)/2} \cos(\theta/2) |011\rangle_{ABC} \\ & + \delta \alpha e^{-i(\varphi-\phi)/2} \sin(\theta/2) |111\rangle_{ABC} \\ & + \delta \beta e^{+i(\varphi+\phi)/2} \cos(\theta/2) |112\rangle_{ABC} \\ & - \delta \beta e^{+i(\varphi-\phi)/2} \sin(\theta/2) |012\rangle_{ABC}. \end{aligned} \quad (75)$$

Bob applies the local operation \mathbf{V}_2 on his qubit and ancillary qutrit:

$$\begin{aligned} \mathbf{V}_2 = & |0\rangle_B \langle 0| \otimes \mathbf{I} \\ & + |1\rangle_B \langle 1| \otimes (|0\rangle_C \langle 1| + |1\rangle_C \langle 2| + |2\rangle_C \langle 0|), \end{aligned} \quad (76)$$

followed by the Hadamard gate \mathbf{H} on the ancillary qutrit to disentangle the ancillary qutrit from Alice's and Bob's qubits. At the end of the protocol, Bob performs the measurement on the ancillary qubit in the computational basis. Let $m = m$ be Bob's measurement outcome with equal probability. Then, the composite state $|\psi_4\rangle_{ABC}$ collapses to

$$\begin{aligned} |\psi_{5m}\rangle_{AB} = & \gamma |\psi\rangle_A |0\rangle_B \\ & + \delta \alpha e^{-i(\varphi+\phi)/2} \cos(\theta/2) |01\rangle_{AB} \\ & + \delta \alpha e^{-i(\varphi-\phi)/2} \sin(\theta/2) |11\rangle_{AB} \\ & + (-1)^m \delta \beta e^{+i(\varphi+\phi)/2} \cos(\theta/2) |11\rangle_{AB} \\ & + (-1)^{\bar{m}} \delta \beta e^{+i(\varphi-\phi)/2} \sin(\theta/2) |01\rangle_{AB}. \end{aligned} \quad (77)$$

Alice and Bob apply the controlled- \mathbf{Z}^m operation in a counterfactual way to transform only

$$|11\rangle_{AB} \rightarrow (-1)^m |11\rangle_{AB}. \quad (78)$$

To implement the set of global flipping operations \mathbf{T} , \mathbf{Q}_1 , \mathbf{Q}_2 , and controlled- \mathbf{Z}^m counterfactually, there is the nonzero probability—called the *abortion rate*—that the physical particle is found in the quantum channel and the protocol fails in counterfactuality. This abortion rate vanishes asymptotically as the cycle numbers of QZ and CQZ gates increase. In case any physical particle is traveled over the quantum channel, Alice and Bob discard the protocol to ensure the full

counterfactuality of CCT. Unless the protocol is discarded, the composite state $|\psi_{5m}\rangle_{AB}$ ends up being the final state

$$\begin{aligned} |\psi_{6m}\rangle_{AB} = & \gamma |\psi\rangle_A |0\rangle_B \\ & + \delta \alpha e^{-i(\varphi+\phi)/2} \cos(\theta/2) |01\rangle_{AB} \\ & + (-1)^m \delta \alpha e^{-i(\varphi-\phi)/2} \sin(\theta/2) |11\rangle_{AB} \\ & + \delta \beta e^{+i(\varphi+\phi)/2} \cos(\theta/2) |11\rangle_{AB} \\ & + (-1)^{\bar{m}} \delta \beta e^{+i(\varphi-\phi)/2} \sin(\theta/2) |01\rangle_{AB} \\ = & \gamma (\mathbf{I} |\psi\rangle_A) \otimes |0\rangle_B + \delta (\mathbf{U}_m |\psi\rangle_A) \otimes |1\rangle_B, \end{aligned} \quad (79)$$

which shows that Bob has successfully performed the CCT on Alice's qubit.

For the unitary teleportation as a special case of the CCT protocol, Bob sets the initial state of his qubit to $|\psi\rangle_B = |1\rangle_B$ leading to

$$|\psi_{6m}\rangle_{AB} = (\mathbf{U}_m |\psi\rangle_A) \otimes |1\rangle_B. \quad (81)$$

Note that (81) shows that at the end of the protocol, the qubits of Alice and Bob are in a separable state, resulting in the unitary transformation of the arbitrary input state $|\psi\rangle_A$ of Alice—also known as the *quantum remote control*.

B. Counterfactual Implementation

Alice and Bob prepare the target and control qubits in their electron and photon. To devise the CCT, Alice and Bob take the following steps (see Fig. 12).

- 1) Bob starts the protocol by throwing his photon towards PBS^H to entangle the polarization (control qubit) state $|\psi\rangle_B$ with the path state $|0\rangle_C$. Then, Alice and Bob have the composite state $|\psi_1\rangle_{ABC}$ in (62).
- 2) Bob passes the horizontal component of the photon to recombine it at the end of the protocol and detours the vertical component of the photon to the 1-CQZ $_{M,N}$ gate. Unless the photon is absorbed, it transforms $|\psi_1\rangle_{ABC}$ to $|\psi_2\rangle_{ABC}$ in (63) with the probability
$$p_1 = f(|\alpha\delta|^2, |\beta\delta|^2). \quad (82)$$
- 3) Bob applies the $\mathbf{B}_1 = \mathbf{R}_z(\varphi) \mathbf{X}$ operation followed by PBS^H on the photon component in the path state $|1\rangle_C$.

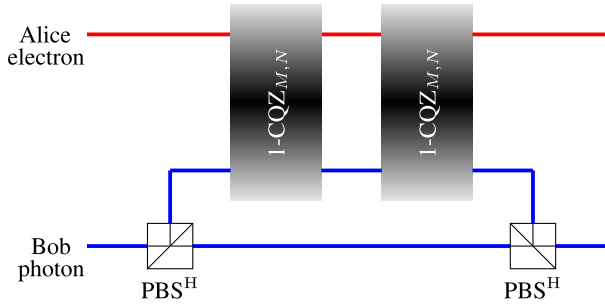


Fig. 13. A counterfactual controlled- Z operator using two $1\text{-CQZ}_{M,N}$ gates concatenated serially.

- 4) Bob applies $\mathcal{B}_2 = R_z(\phi) R_y(\theta)$ and $\mathcal{B}_3 = X\mathcal{B}_2$ operators on the photon components in the path states $|1\rangle_C$ and $|2\rangle_C$, respectively. Then, the composite state of Alice and Bob transforms to $|\psi_3\rangle_{ABC}$ in (72).
- 5) To apply \mathcal{Q}_1 counterfactually, Bob inputs the photon components in path states $|1\rangle_C$ and $|2\rangle_C$ to the D-DCF $_{K,N}$ gate. From (56), unless the photon is absorbed by the electron in the D-DCF $_{K,N}$ gate, it transforms $|\psi_3\rangle_{ABC}$ as follows:

$$\begin{aligned} |\psi_{31}\rangle_{ABC} = & \gamma (\alpha |1\rangle_A - \beta |0\rangle_A) |00\rangle_{BC} \\ & - \delta \alpha e^{-i(\varphi+\phi)/2} \cos(\theta/2) |111\rangle_{ABC} \\ & + \delta \alpha e^{-i(\varphi-\phi)/2} \sin(\theta/2) |001\rangle_{ABC} \\ & - \delta \beta e^{i(\varphi+\phi)/2} \cos(\theta/2) |012\rangle_{ABC} \\ & - \delta \beta e^{i(\varphi-\phi)/2} \sin(\theta/2) |102\rangle_{ABC} \end{aligned} \quad (83)$$

with the probability

$$p_2 = g (|\delta|^2 \sin^2(\theta/2)). \quad (84)$$

Now, Alice applies ZX on her qubit and Bob performs the Z operation on path states $|1\rangle_C$ and $|2\rangle_C$ to complete the \mathcal{Q}_1 operation.

- 6) To apply \mathcal{Q}_2 counterfactually, Bob inputs the photon components in path states $|1\rangle_C$ and $|2\rangle_C$ to the $1\text{-CQZ}_{M,N}$ and $0\text{-CQZ}_{M,N}$ gates in the D-CQZ $_{M,N}$ gate, respectively. Unless the photon is discarded in the D-CQZ $_{M,N}$ gate, Bob locally applies the X operator on the photon component in the path state $|2\rangle_C$ to complete the \mathcal{Q}_2 operation. From (38), the composite state of Alice and Bob transforms to $|\psi_4\rangle_{ABC}$ in (75) with the probability

$$\begin{aligned} p_3 = & f (|\delta\alpha|^2 \cos^2(\theta/2) + |\delta\beta|^2 \sin^2(\theta/2), \\ & |\delta\beta|^2 \cos^2(\theta/2) + |\delta\alpha|^2 \sin^2(\theta/2)). \end{aligned} \quad (85)$$

- 7) To disentangle the ancillary qutrit, Bob applies the local operation V_2 followed by the Hadamard gate H on the ancilla and performs the measurement on the ancilla in the computational basis. It collapses the composite state $|\psi_4\rangle_{ABC}$ to $|\psi_{5m}\rangle_{AB}$ in (77).
- 8) Alice and Bob perform the controlled- Z^m operation depending on the measurement result m . For $m = 1$, Bob applies PBS^H again and inputs the component of the photon in the path state $|1\rangle_C$ to $1\text{-CQZ}_{M,N}$ gates. Since

$$\begin{aligned} & 1\text{-CQZ}_{M,N} (1\text{-CQZ}_{M,N} (|c_{qz1}\rangle_{AB})) \\ & = \text{CPHASE} |c_{qz1}\rangle_{AB} \end{aligned} \quad (86)$$

with the probability λ_2^2 , Alice and Bob apply two $1\text{-CQZ}_{M,N}$ gates in series to perform the controlled- Z operation counterfactually as shown in Fig. 13. At the end of the protocol, Bob recombines the horizontal and vertical components of the photon, and the composite state of Alice and Bob transforms to $|\psi_{6m}\rangle_{AB}$ in (79) with the probability

$$p_4^m = f^{2m} (|\alpha\gamma|^2, |\beta\gamma|^2). \quad (87)$$

In the CCT protocol for general input states, the success probability (i.e., the complement of the abortion rate) P_m is given as

$$P_m = p_1 p_2 p_3 p_4^m, \quad (88)$$

which tends to one as $M, N, K \rightarrow \infty$ (see Fig. 14). Here, it is important to note that the success probability of the CCT protocol increases as M, N , and K go to infinity. However, it reduces the stability of the nested Mach-Zehnder interferometer. This problem may limit the success probability of the CCT protocol and needs to be overcome in future work towards effective CCT.

C. CCT Protocols for Bell-Type States

Let the entangled states

$$|\mathfrak{B}_{ab}\rangle_{AB} = \alpha |ab\rangle_{AB} + \beta |\bar{a}\bar{b}\rangle_{AB} \quad (89)$$

be Bell-type states. Note that $|\mathfrak{B}_{0\ell}\rangle_{AB}$ and its swapped state

$$\begin{aligned} |\mathfrak{B}_{\ell 0}\rangle_{AB} &= \text{SWAP} |\mathfrak{B}_{0\ell}\rangle_{AB} \\ &= \alpha |\ell 0\rangle_{AB} + \beta |\bar{\ell} 1\rangle_{AB} \end{aligned} \quad (90)$$

are called the ℓ -class Bell-type states in the paper.

1) Protocol: Consider that the initial states of Alice and Bob are ℓ -class Bell-type states

$$|\psi_0\rangle_{AB} = |\mathfrak{B}_{\ell 0}\rangle_{AB} \quad (91)$$

and Bob knows the value of ℓ . Similar to the general input state, Bob starts the protocol by entangling his qubit with the ancillary qubit $|0\rangle_C$ (see Fig. 15). Now, Bob directly applies

$$\tilde{V}_1(U) = I \otimes |0\rangle_C \langle 0| + (X^\ell U X^\ell) \otimes |1\rangle_C \langle 1| \quad (92)$$

for the ℓ -class states. Alice and Bob counterfactually apply

$$\begin{aligned} \tilde{Q}_1 = & I \otimes (|00\rangle_{BC} \langle 00| + |10\rangle_{BC} \langle 10| \\ & + (-1)^\ell |11\rangle_{BC} \langle 11|) + (-1)^\ell X \otimes |01\rangle_{BC} \langle 01|, \end{aligned} \quad (93)$$

followed by

$$\begin{aligned} \tilde{Q}_2 = & (|0\rangle_A \langle 0| + |1\rangle_A \langle 1|) \otimes I \otimes |0\rangle_C \langle 0| \\ & + (-1)^\ell |1\rangle_A \langle 1| \otimes X^\ell \otimes |1\rangle_C \langle 1| \\ & + (-1)^\ell |0\rangle_A \langle 0| \otimes X^{\bar{\ell}} \otimes |1\rangle_C \langle 1| \end{aligned} \quad (94)$$

for the ℓ -class states. At the end of the protocol, Bob applies the local CNOT operation at his qubits to disentangle the ancillary qubit. Again, there exists the abortion rate that the physical particle is transmitted over the quantum channel and the protocol fails to implement the set of global flipping operations \tilde{Q}_1 and \tilde{Q}_2 counterfactually—which tends to zero

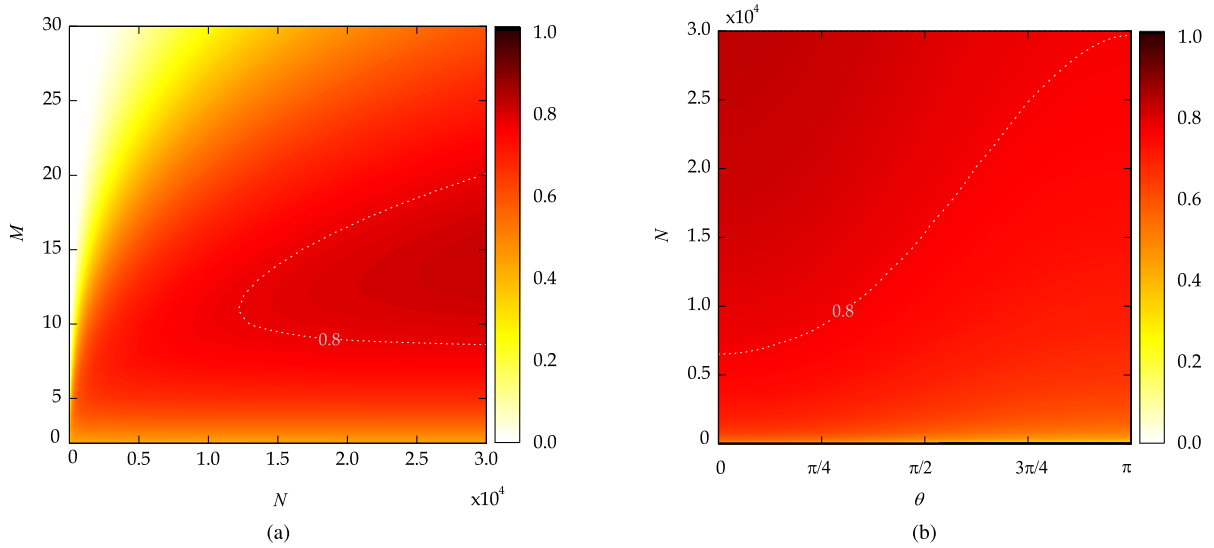


Fig. 14. (a) Success probability P_m as a function of M and N for general input states when $K = M$, $\theta = \pi/4$, and $|\alpha|^2 = |\gamma|^2 = 1/2$. Since the success probability P_m is concave in $M > 1$, for any positive integer N , there exists the optimal value M that maximizes the success probability for a given N . (b) Success probability P_m as a function of N and θ when $M = \arg \max P_m$ for given N , $K = M$, and $|\alpha|^2 = |\gamma|^2 = 1/2$.

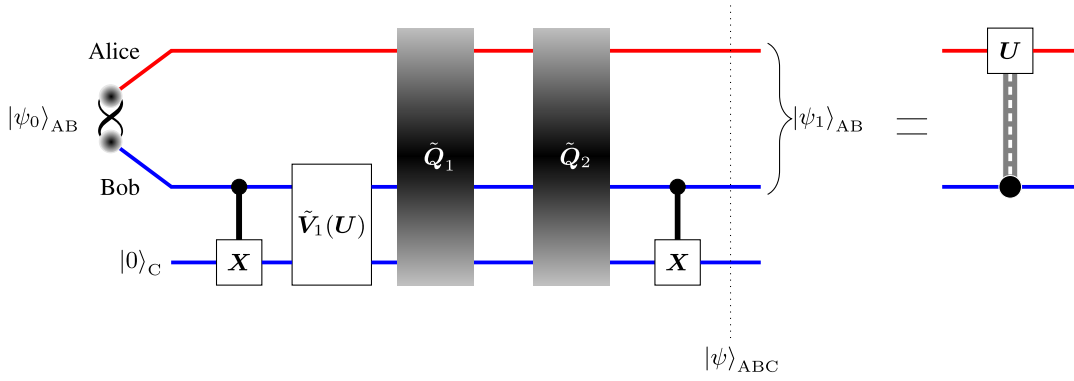


Fig. 15. A deterministic CCT protocol for Bell-type states to counterfactually apply U on Alice's qubit in a concealed and controlled fashion without using additional preshared entanglement. Similar to the CCT protocol for general input states, Bob starts the protocol by entangling his qubit with ancilla $|0\rangle_C$ with the local CNOT operation. Alice and Bob apply a sequence of nonlocal controlled flipping operations \tilde{Q}_1 , \tilde{Q}_2 and the local operation $\tilde{V}_1(U)$ (at Bob's side). At the end of the protocol, Bob applies the CNOT operation locally to disentangle the ancilla qubit and transforms the composite state as $|\psi\rangle_{ABC} = (\mathbf{I} \otimes |0\rangle_B \langle 0| + U \otimes |1\rangle_B \langle 1|) |\psi_0\rangle_{AB} \otimes |0\rangle_C$.

under the asymptotic limits. Unless the protocol is discarded, the CCT protocol for Bell-type states transforms $|\psi_0\rangle_{AB}$ as follows:

$$|\psi\rangle_{ABC} = |\psi_1\rangle_{AB} \otimes |0\rangle_C, \quad (95)$$

where

$$|\psi_1\rangle_{AB} = (\mathbf{I} \otimes |0\rangle_B \langle 0| + U \otimes |1\rangle_B \langle 1|) |\psi_0\rangle_{AB}. \quad (96)$$

As the ancillary qubit is already in a separable state with qubits A and B, Bob does not need to perform measurements on his ancillary qubit.

2) *Counterfactual Implementation*: To demonstrate the CCT implementation for Bell-type states, Alice and Bob prepare the composite input state $|\psi_0\rangle_{AB} = |\mathfrak{B}_{\ell 0}\rangle_{AB}$ in the electron-photon pair. Similar to the general setup, Bob starts the protocol by applying PBS^H on his photon, as shown in Fig. 16. The CCT protocol for ℓ -class Bell-type states takes the following steps.

1) Bob applies $\tilde{\mathfrak{B}}_1 = \mathbf{X}^\ell U \mathbf{X}^\ell$ on the component of the photon in the path state $|1\rangle_C$ for ℓ -class states.

2) To apply \tilde{Q}_1 counterfactually, Bob inputs the photon components in the path state $|1\rangle_C$ to the $\bar{\ell}$ -DCF $_{K,N}$ gate for ℓ -class states. From (51), unless the photon is absorbed in the $\bar{\ell}$ -DCF $_{K,N}$ gate, it transforms the composite state of Alice and Bob as follows:

$$\begin{aligned} |\psi_{01}\rangle_{ABC} &= (-1)^\ell \alpha |\bar{\ell}00\rangle_{ABC} \\ &\quad - \beta \cos(\theta/2) |\ell 11\rangle_{ABC} \\ &\quad + (-1)^{\bar{\ell}} \beta \sin(\theta/2) |\bar{\ell} 11\rangle_{ABC} \end{aligned} \quad (97)$$

with the probability

$$p_5 = g(|\beta|^2 \sin^2(\theta/2)). \quad (98)$$

Now, Alice applies $\mathbf{Z}\mathbf{X}$ on her qubit to complete the \tilde{Q}_1 operation.

3) To apply \tilde{Q}_2 counterfactually, Bob applies $\tilde{\mathfrak{B}}_2 = \mathbf{X}^{\bar{\ell}} \mathbf{Z}$ operation on the components of the photon in the path state $|1\rangle_C$ for ℓ -class states. Now, Bob inputs the respective component of the photon to the 1-CQZ $_{M,N}$

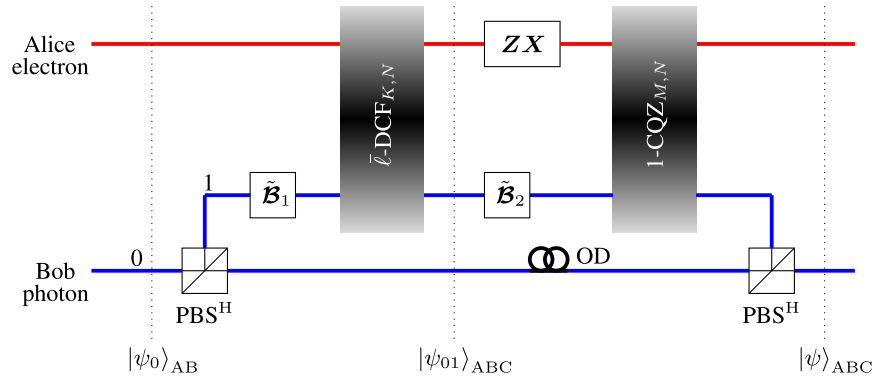


Fig. 16. A CCT protocol for ℓ -class Bell-type states using the $\bar{\ell}$ -DCF $_{K,N}$ gate where $\tilde{\mathcal{B}}_1 = \mathbf{X}^\ell \mathbf{U} \mathbf{X}^\ell$ and $\tilde{\mathcal{B}}_2 = \mathbf{X}^{\bar{\ell}} \mathbf{Z}$ for ℓ -class states.

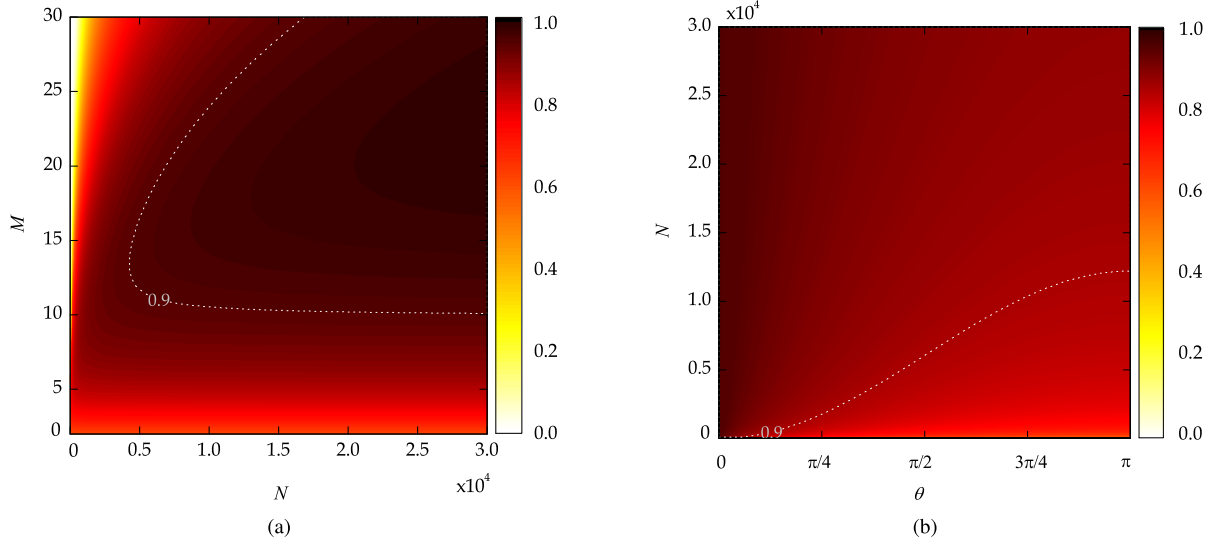


Fig. 17. (a) Success probability P as a function of M and N for Bell-type input states when $K = M$, $\theta = \pi/4$, and $|\alpha|^2 = 1/2$. Since the success probability P is concave in $M > 1$, for any positive integer N , there exists the optimal value M that maximizes the success probability for a given N . (b) Success probability P as a function of N and θ when $M = \arg \max P$ for given N , $K = M$, and $|\alpha|^2 = 1/2$.

gate to complete the $\tilde{\mathcal{Q}}_2$ operation. At the end of the protocol, unless the photon is absorbed by the electron in the 1-CQZ $_{M,N}$ gate, Bob recombines the horizontal and vertical components of the photon and the composite state $|\psi_{01}\rangle_{ABC}$ transforms to $|\psi_1\rangle_{ABC}$ in (95) with the probability

$$p_6 = f(|\beta|^2 \cos^{2\ell}(\theta/2) \sin^{2\bar{\ell}}(\theta/2), |\beta|^2 \sin^{2\ell}(\theta/2) \cos^{2\bar{\ell}}(\theta/2)) \quad (99)$$

for ℓ -class states.

For the CCT protocol with Bell-type states, the success probability P is given by

$$P = p_5 p_6 \quad (100)$$

tending again to one as $M, N, K \rightarrow \infty$ (see Fig. 17).

D. Numerical Examples

We exemplify the quantum anonymous broadcast network using the CCT protocol. In contrast to the original anonymous quantum protocol in [5], the cloud server locally prepares an n -qubit GHZ state. To anonymously broadcast classical

information, the edge server i applies the unitary operation $U_{(i)}$ on the i^{th} qubit of the cloud server using the CCT protocol in a counterfactual and concealed manner where $U_{(i)} = \mathbf{I}$ for all $i \in \{1, 2, \dots, n\}$ and $i \neq s$. For the edge server s , the unitary operation $U_{(s)}$ carries classical information to be broadcasted anonymously. At the end of the protocol, the cloud server performs the measurement on its respective qubits and broadcasts the decoded classical information. From [5], the degree of anonymity \mathcal{D}_A for the quantum anonymous broadcast network with the CCT protocol is given as

$$\mathcal{D}_A = -\frac{P_m \log_2(n-r)}{\log_2(n)}, \quad (101)$$

where r denotes the number of dishonest servers. Note that the dependence of \mathcal{D}_A on M, N , and K is from P_m . Fig. 18 shows \mathcal{D}_A for the quantum anonymous broadcast network with the CCT protocol. It can be seen that due to the non-zero abortion rate of the CCT protocol, \mathcal{D}_A is not equal to one even if there are no dishonest edge servers in the network. Here, it is important that Fig. 18 shows numerical results for a qubit system. However, the CCT protocol can be employed

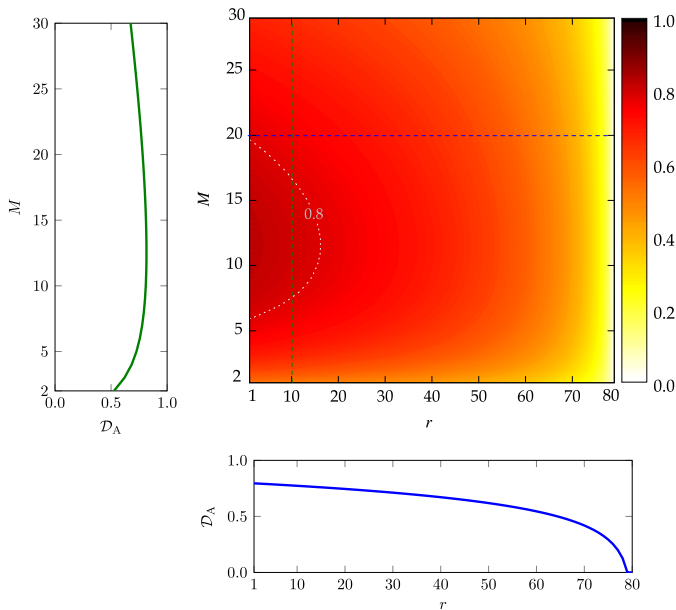


Fig. 18. The degree of anonymity \mathcal{D}_A for the quantum anonymous broadcast network using the CCT protocol as a function of M and the number of dishonest servers r when $K = M$, $N = 1000 \times M$, and $\theta = \pi/4$. The blue solid line is the trajectory of \mathcal{D}_A as a function of r for $M = 20$, whereas the left plot depicts \mathcal{D}_A as a function of M when $r = 10$. We also plot the trajectory of (M, r) achieving the degree of anonymity of 0.8 (white dashed line).

for a 2^d dimensional qudit system where unitary operations can be considered as d -qubit transformations which can be decomposed into the multiplication of single-qubit and two-qubit unitary operations.

V. CONCLUSION

We have devised a new protocol for distributed quantum computing that allows Alice and Bob to apply a two-qubit controlled unitary operator on any input state in a probabilistic fashion without using preshared entanglement, without revealing the unitary operator to Alice, and without exchanging physical particles between remote parties. As (i) any n -qubit unitary operator can be decomposed into the product of two-qubit unitary operators and single-qubit operators; and (ii) the controlled flipping operators Q_1 and Q_2 are independent of the input states, the CCT protocol can play an important role in quantum-federated learning to achieve 6G URLLC and ensure data security. Furthermore, the concealed nature of the proposed protocol enables Bob to appeal quantum remote control at a distinct party in a cryptographic manner in emerging wireless networks. As an example, we have simulated CCT protocols for quantum anonymous networks. Future work may consider suitable variations of the proposed protocols for various other cryptographic tasks, such as quantum-secret sharing in 6G networks.

REFERENCES

[1] J. Park et al., "Extreme ultra-reliable and low-latency communication," *Nature Electron.*, vol. 5, no. 3, pp. 133–141, Mar. 2022.
 [2] C. She et al., "A tutorial on ultrareliable and low-latency communications in 6G: Integrating domain knowledge into deep learning," *Proc. IEEE*, vol. 109, no. 3, pp. 204–246, Mar. 2021.

[3] S. Samarakoon, M. Bennis, W. Saad, and M. Debbah, "Distributed federated learning for ultra-reliable low-latency vehicular communications," *IEEE Trans. Commun.*, vol. 68, no. 2, pp. 1146–1159, Feb. 2020.
 [4] W. Xia, W. Wen, K. Wong, T. Q. S. Quek, J. Zhang, and H. Zhu, "Federated-learning-based client scheduling for low-latency wireless communications," *IEEE Wireless Commun.*, vol. 28, no. 2, pp. 32–38, Apr. 2021.
 [5] A. Khan, U. Khalid, J. U. Rehman, and H. Shin, "Quantum anonymous private information retrieval for distributed networks," *IEEE Trans. Commun.*, vol. 70, no. 6, pp. 4026–4037, Jun. 2022.
 [6] A. Khan, U. Khalid, J. U. Rehman, K. Lee, and H. Shin, "Quantum anonymous collision detection for quantum networks," *EPJ Quantum Technol.*, vol. 8, no. 1, p. 27, Dec. 2021.
 [7] A. Khan, J. U. Rehman, and H. Shin, "Quantum anonymous notification for network-based applications," *Quantum Inf. Process.*, vol. 20, no. 12, p. 397, Nov. 2021.
 [8] V. Giovannetti, L. Maccone, T. Morimae, and T. G. Rudolph, "Efficient universal blind quantum computation," *Phys. Rev. Lett.*, vol. 111, no. 23, Dec. 2013, Art. no. 230501.
 [9] C. A. Pérez-Delgado and J. F. Fitzsimons, "Iterated gate teleportation and blind quantum computation," *Phys. Rev. Lett.*, vol. 114, no. 22, Jun. 2015, Art. no. 220502.
 [10] J. F. Fitzsimons, "Private quantum computation: An introduction to blind quantum computing and related protocols," *NPJ Quantum Inf.*, vol. 3, no. 1, pp. 1–11, Jun. 2017.
 [11] W. Li, S. Lu, and D.-L. Deng, "Quantum federated learning through blind quantum computing," *Sci. China Phys., Mech. Astron.*, vol. 64, no. 10, pp. 1–8, Sep. 2021.
 [12] F. Zaman, A. Farooq, M. A. Ullah, H. Jung, H. Shin, and M. Z. Win, "Quantum machine intelligence for 6G URLLC," *IEEE Wireless Commun.*, vol. 30, no. 2, pp. 22–30, Apr. 2023.
 [13] J. I. Cirac, A. K. Ekert, S. F. Huelga, and C. Macchiavello, "Distributed quantum computation over noisy channels," *Phys. Rev. A, Gen. Phys.*, vol. 59, no. 6, pp. 4249–4254, Jun. 1999.
 [14] W. Dai, T. Peng, and M. Z. Win, "Optimal remote entanglement distribution," *IEEE J. Sel. Areas Commun.*, vol. 38, no. 3, pp. 540–556, Mar. 2020.
 [15] A. S. Cacciapuoti, M. Caleffi, F. Tafuri, F. S. Cataliotti, S. Gherardini, and G. Bianchi, "Quantum internet: Networking challenges in distributed quantum computing," *IEEE Netw.*, vol. 34, no. 1, pp. 137–143, Jan. 2020.
 [16] J. Eisert, K. Jacobs, P. Papadopoulos, and M. B. Plenio, "Optimal local implementation of nonlocal quantum gates," *Phys. Rev. A, Gen. Phys.*, vol. 62, no. 5, Oct. 2000, Art. no. 052317.
 [17] A. S. Fletcher, P. W. Shor, and M. Z. Win, "Channel-adapted quantum error correction for the amplitude damping channel," *IEEE Trans. Inf. Theory*, vol. 54, no. 12, pp. 5705–5718, Dec. 2008.
 [18] M. Chiani, A. Conti, and M. Z. Win, "Piggybacking on quantum streams," *Phys. Rev. A, Gen. Phys.*, vol. 102, no. 1, Jul. 2020, Art. no. 012410.
 [19] L. Chen and L. Yu, "Decomposition of bipartite and multipartite unitary gates into the product of controlled unitary gates," *Phys. Rev. A, Gen. Phys.*, vol. 91, no. 3, Mar. 2015, Art. no. 032308.
 [20] A. Barenco et al., "Elementary gates for quantum computation," *Phys. Rev. A, Gen. Phys.*, vol. 52, no. 5, pp. 3457–3467, Nov. 1995.
 [21] A. Soeda, P. S. Turner, and M. Murao, "Entanglement cost of implementing controlled-unitary operations," *Phys. Rev. Lett.*, vol. 107, no. 18, Oct. 2011, Art. no. 180501.
 [22] K. Lemr, K. Bartkiewicz, A. Černoč, M. Dušek, and J. Soubusta, "Experimental implementation of optimal linear-optical controlled-unitary gates," *Phys. Rev. Lett.*, vol. 114, no. 15, Apr. 2015, Art. no. 153602.
 [23] Y. Liu et al., "Experimental demonstration of counterfactual quantum communication," *Phys. Rev. Lett.*, vol. 109, no. 3, Jul. 2012, Art. no. 030501.
 [24] H. Salih, Z.-H. Li, M. Al-Amri, and M. S. Zubairy, "Protocol for direct counterfactual quantum communication," *Phys. Rev. Lett.*, vol. 110, no. 17, Apr. 2013, Art. no. 170502.
 [25] Y. Aharonov and L. Vaidman, "Modification of counterfactual communication protocols that eliminates weak particle traces," *Phys. Rev. A, Gen. Phys.*, vol. 99, no. 1, Jan. 2019, Art. no. 010103.
 [26] Y. Aharonov and D. Rohrlich, "What is nonlocal in counterfactual quantum communication?" *Phys. Rev. Lett.*, vol. 125, no. 26, Dec. 2020, Art. no. 260401.

- [27] F. Zaman, K. Lee, and H. Shin, "Information carrier and resource optimization of counterfactual quantum communication," *Quantum Inf. Process.*, vol. 20, no. 5, pp. 1–10, May 2021.
- [28] Y. Aharonov, E. Cohen, and S. Popescu, "A dynamical quantum cheshire cat effect and implications for counterfactual communication," *Nature Commun.*, vol. 12, no. 1, pp. 1–8, Aug. 2021.
- [29] W. M. Itano, D. J. Heinzen, J. J. Bollinger, and D. Wineland, "Quantum Zeno effect," *Phys. Rev. A, Gen. Phys.*, vol. 41, no. 5, p. 2295, Mar. 1990.
- [30] P. Kwiat, H. Weinfurter, T. Herzog, A. Zeilinger, and M. A. Kasevich, "Interaction-free measurement," *Phys. Rev. Lett.*, vol. 74, no. 24, p. 4763, Nov. 1995.
- [31] P. G. Kwiat et al., "High-efficiency quantum interrogation measurements via the quantum Zeno effect," *Phys. Rev. Lett.*, vol. 83, no. 23, pp. 4725–4728, Dec. 1999.
- [32] Y. Chen, D. Jian, X. Gu, L. Xie, and L. Chen, "Counterfactual entanglement distribution using quantum dot spins," *J. Opt. Soc. Amer. B, Opt. Phys., Opt. Phys.*, vol. 33, no. 4, pp. 663–669, Jan. 2016.
- [33] F. Zaman, Y. Jeong, and H. Shin, "Counterfactual bell-state analysis," *Sci. Rep.*, vol. 8, no. 1, p. 14641, Oct. 2018.
- [34] O. Hosten, M. T. Rakher, J. T. Barreiro, N. A. Peters, and P. G. Kwiat, "Counterfactual quantum computation through quantum interrogation," *Nature*, vol. 439, no. 7079, pp. 949–952, Feb. 2006.
- [35] F. Zaman, Y. Jeong, and H. Shin, "Dual quantum Zeno superdense coding," *Sci. Rep.*, vol. 9, no. 1, p. 11193, Aug. 2019.
- [36] F. Kong et al., "Experimental realization of high-efficiency counterfactual computation," *Phys. Rev. Lett.*, vol. 115, no. 8, Aug. 2015, Art. no. 080501.
- [37] F. Zaman, E.-K. Hong, and H. Shin, "Local distinguishability of bell-type states," *Quantum Inf. Process.*, vol. 20, no. 5, pp. 1–12, May 2021.
- [38] I. A. Calafell et al., "Trace-free counterfactual communication with a nanophotonic processor," *NPJ Quantum Inf.*, vol. 5, no. 1, pp. 1–5, Jul. 2019.
- [39] Y. Cao et al., "Direct counterfactual communication via quantum Zeno effect," *Proc. Nat. Acad. Sci. USA*, vol. 114, no. 19, pp. 4920–4924, May 2017.
- [40] S. Yun, K. Kwon, J. U. Rehman, F. Zaman, and H. Shin, "Quantum duplex coding for classical information on IBM quantum devices," in *Proc. Korean Inst. Commun. Inf. Sci. (KICS) Autumn Conf.*, Nov. 2019, pp. 415–418.
- [41] F. Zaman, H. Shin, and M. Z. Win, "Counterfactual full-duplex communication," 2019, *arXiv:1910.03200*.
- [42] Z.-H. Li, M. Al-Amri, X.-H. Yang, and M. S. Zubairy, "Counterfactual exchange of unknown quantum states," *Phys. Rev. A, Gen. Phys.*, vol. 100, no. 2, Aug. 2019, Art. no. 022110.
- [43] F. Zaman and H. Shin, "Counterfactual Swap gates," in *Proc. Korean Inst. Commun. Inf. Sci. (KICS) Winter Conf.*, pp. 389–390, Feb. 2021.
- [44] Z.-H. Li, M. Al-Amri, and M. S. Zubairy, "Direct counterfactual transmission of a quantum state," *Phys. Rev. A, Gen. Phys.*, vol. 92, no. 5, Nov. 2015, Art. no. 052315.
- [45] Q. Guo, L.-Y. Cheng, L. Chen, H.-F. Wang, and S. Zhang, "Counterfactual quantum-information transfer without transmitting any physical particles," *Sci. Rep.*, vol. 5, no. 1, pp. 1–6, Feb. 2015.
- [46] T.-G. Noh, "Counterfactual quantum cryptography," *Phys. Rev. Lett.*, vol. 103, no. 23, Dec. 2009, Art. no. 230501.
- [47] H. Salih, "Tripartite counterfactual quantum cryptography," *Phys. Rev. A, Gen. Phys.*, vol. 90, no. 1, Jul. 2014, Art. no. 012333.
- [48] F. Zaman, Y. Jeong, and H. Shin, "Man in the middle attack in counterfactual quantum key distribution," in *Proc. Korean Inst. Commun. Inf. Sci. (KICS) Autumn Conf.*, Nov. 2018, pp. 105–106.
- [49] Z.-Q. Yin et al., "Counterfactual quantum cryptography based on weak coherent states," *Phys. Rev. A, Gen. Phys.*, vol. 86, no. 2, Aug. 2012, Art. no. 022313.
- [50] S. N. Paing, F. Zaman, and H. Shin, "Counterfactual controlled quantum teleportation," in *Proc. Korean Inst. Commun. Inf. Sci. (KICS) Winter Conf.*, Feb. 2021, pp. 542–543.
- [51] S. N. Paing, F. Zaman, and H. Shin, "Counterfactual quantum private comparison," in *Proc. Korean Inst. Commun. Inf. Sci. (KICS) Winter Conf.*, Feb. 2022, pp. 651–653.
- [52] H. Salih, J. R. Hance, W. McCutcheon, T. Rudolph, and J. Rarity, "Exchange-free computation on an unknown qubit at a distance," *New J. Phys.*, vol. 23, no. 1, Jan. 2021, Art. no. 013004.
- [53] Z. Cao, "Counterfactual universal quantum computation," *Phys. Rev. A, Gen. Phys.*, vol. 102, no. 5, Nov. 2020, Art. no. 052413.
- [54] R. Chen, C. Li, S. Yan, R. Malaney, and J. Yuan, "Physical layer security for ultra-reliable and low-latency communications," *IEEE Wireless Commun.*, vol. 26, no. 5, pp. 6–11, Oct. 2019.
- [55] Z. Hou, C. She, Y. Li, D. Niyato, M. Dohler, and B. Vucetic, "Intelligent communications for tactile internet in 6G: Requirements, technologies, and challenges," *IEEE Commun. Mag.*, vol. 59, no. 12, pp. 82–88, Dec. 2021.
- [56] M. Alsabah et al., "6G wireless communications networks: A comprehensive survey," *IEEE Access*, vol. 9, pp. 148191–148243, 2021.
- [57] A. D. Ijala, S. Thomas, O. Oshiga, S. U. Hussein, T. Karataev, and O. Osanaiye, "A review of vision and challenges of the 6G wireless networks," in *Proc. 1st Int. Conf. Multidisciplinary Eng. Appl. Sci. (ICMEAS)*, Jul. 2021, pp. 1–6.
- [58] A. A. Nasir, H. D. Tuan, T. Q. Duong, and H. V. Poor, "Secrecy rate beamforming for multicell networks with information and energy harvesting," *IEEE Trans. Signal Process.*, vol. 65, no. 3, pp. 677–689, Feb. 2017.
- [59] J. Zhang et al., "Experimental study on key generation for physical layer security in wireless communications," *IEEE Access*, vol. 4, pp. 4464–4477, 2016.
- [60] R. Horodecki, P. Horodecki, M. Horodecki, and K. Horodecki, "Quantum entanglement," *Rev. Mod. Phys.*, vol. 81, p. 865, Jun. 2009.
- [61] N. Linden, S. Popescu, A. J. Short, and A. Winter, "Quantum nonlocality and beyond: Limits from nonlocal computation," *Phys. Rev. Lett.*, vol. 99, no. 18, Oct. 2007, Art. no. 180502.
- [62] W. K. Wootters and W. H. Zurek, "A single quantum cannot be cloned," *Nature*, vol. 299, no. 5886, pp. 802–803, Oct. 1982.
- [63] Z. Quan and T. Chaojing, "Simple proof of the unconditional security of the Bennett 1992 quantum key distribution protocol," *Phys. Rev. A, Gen. Phys.*, vol. 65, no. 6, May 2002, Art. no. 062301.
- [64] S. D. Bartlett, T. Rudolph, and R. W. Spekkens, "Reference frames, superselection rules, and quantum information," *Rev. Mod. Phys.*, vol. 79, no. 2, pp. 555–609, Apr. 2007.
- [65] E. O. Ilo-Okeke, L. Tessler, J. P. Dowling, and T. Byrnes, "Remote quantum clock synchronization without synchronized clocks," *NPJ Quantum Inf.*, vol. 4, no. 1, pp. 1–5, Aug. 2018.
- [66] K. Boström and T. Felbinger, "Deterministic secure direct communication using entanglement," *Phys. Rev. Lett.*, vol. 89, no. 18, Oct. 2002, Art. no. 187902.
- [67] J.-Y. Hu et al., "Experimental quantum secure direct communication with single photons," *Light, Sci. Appl.*, vol. 5, no. 9, Apr. 2016, Art. no. e16144.
- [68] S. Qaisar, J. U. Rehman, Y. Jeong, and H. Shin, "Practical deterministic secure quantum communication in a lossy channel," *Prog. Theor. Experim. Phys.*, vol. 2017, no. 4, p. 41, Apr. 2017.
- [69] L. Ruan, W. Dai, and M. Z. Win, "Adaptive recurrence quantum entanglement distillation for two-Kraus-operator channels," *Phys. Rev. A, Gen. Phys.*, vol. 97, no. 5, May 2018, Art. no. 052332.
- [70] A. Khan, A. Farooq, Y. Jeong, and H. Shin, "Distribution of entanglement in multipartite systems," *Quantum Inf. Process.*, vol. 18, no. 2, p. 60, Jan. 2019.
- [71] Z.-H. Li, L. Wang, J. Xu, Y. Yang, M. Al-Amri, and M. S. Zubairy, "Counterfactual trojan horse attack," *Phys. Rev. A, Gen. Phys.*, vol. 101, Feb. 2020, Art. no. 022336.
- [72] C. B. Chiu, E. C. G. Sudarshan, and B. Misra, "Time evolution of unstable quantum states and a resolution of Zeno's paradox," *Phys. Rev. D, Part. Fields*, vol. 16, no. 2, pp. 520–529, Jul. 1977.
- [73] R. Omnès, "Consistent interpretations of quantum mechanics," *Rev. Mod. Phys.*, vol. 64, no. 2, pp. 339–382, Apr. 1992.
- [74] P. Facchi and S. Pascazio, "Quantum Zeno subspaces," *Phys. Rev. Lett.*, vol. 89, no. 8, Aug. 2002, Art. no. 080401.
- [75] S. Morley-Short, L. Rosenfeld, and P. Kok, "Unitary evolution and the distinguishability of quantum states," *Phys. Rev. A, Gen. Phys.*, vol. 90, no. 6, Dec. 2014, Art. no. 062116.
- [76] K. Koshino and A. Shimizu, "Quantum Zeno effect by general measurements," *Phys. Rep.*, vol. 412, no. 4, pp. 191–275, Jun. 2005.
- [77] P. Facchi, H. Nakazato, and S. Pascazio, "From the quantum Zeno to the inverse quantum Zeno effect," *Phys. Rev. Lett.*, vol. 86, no. 13, pp. 2699–2703, Mar. 2001.
- [78] M. B. Plenio and P. L. Knight, "The quantum-jump approach to dissipative dynamics in quantum optics," *Rev. Mod. Phys.*, vol. 70, no. 1, pp. 101–144, Jan. 1998.
- [79] B. Kaulakys and V. Gontis, "Quantum anti-Zeno effect," *Phys. Rev. A, Gen. Phys.*, vol. 56, no. 2, pp. 1131–1137, Aug. 1997.

- [80] A. P. Balachandran and S. M. Roy, "Quantum anti-Zeno paradox," *Phys. Rev. Lett.*, vol. 84, no. 18, pp. 4019–4022, May 2000.
- [81] O. V. Prezhdo, "Quantum anti-Zeno acceleration of a chemical reaction," *Phys. Rev. Lett.*, vol. 85, no. 21, pp. 4413–4417, Nov. 2000.
- [82] R. H. Dicke, "Interaction-free quantum measurements: A paradox?" *Amer. J. Phys.*, vol. 49, no. 10, pp. 925–930, Oct. 1981.
- [83] A. Elitzur and L. Vaidman, "Quantum mechanical interaction-free measurement," *Found. Phys.*, vol. 23, no. 76, pp. 987–997, Jul. 1993.
- [84] E. H. du Marchie van Voorthuysen, "Realization of an interaction-free measurement of the presence of an object in a light beam," *Amer. J. Phys.*, vol. 64, no. 12, pp. 1504–1507, Dec. 1996.



Fakhar Zaman (Student Member, IEEE) received the B.E. degree in electrical engineering from the National University of Sciences and Technology (NUST), Pakistan, in 2015. He is currently pursuing the Ph.D. degree in quantum information science with the Department of Electronics and Information Convergence Engineering, Kyung Hee University (KHU), South Korea.

He is currently a Graduate Research Scholar with the Communications and Quantum Information Laboratory, KHU, and an Exchange Visiting Student

with the Wireless Information and Network Sciences Laboratory, Massachusetts Institute of Technology (MIT). His research interests include quantum control, remote entanglement distribution, and deep reinforcement learning.

Mr. Zaman was a recipient of the Best Paper Award at the KICS-Fall Conference on Communications, in 2019. He served as a Reviewer for the IEEE JOURNAL ON SELECTED AREAS IN COMMUNICATIONS and several international conferences.



Saw Nang Paing received the B.E. degree in computer engineering and information technology from Mandalay Technology University (MTU), Myanmar, in 2019. She is currently pursuing the Ph.D. degree in quantum information science with the Department of Electronics and Information Convergence Engineering, Kyung Hee University (KHU), South Korea. Her research interests include distributed quantum networks, quantum communication, and quantum security.



Ahmad Farooq received the B.S. degree in electronics engineering from the Ghulam Ishaq Khan (GIK) Institute, Topi, Pakistan, in 2015, and the Ph.D. degree in electronic engineering from Kyung Hee University, South Korea, in 2022. Since 2022, he has been a Post-Doctoral Fellow with the Department of Electronic Engineering, Kyung Hee University. His research interests include quantum information science, quantum computing, and quantum estimation theory.



Hyundong Shin (Fellow, IEEE) received the B.S. degree in Electronics Engineering from Kyung Hee University (KHU), Yongin-si, Korea, in 1999, and the M.S. and Ph.D. degrees in Electrical Engineering from Seoul National University, Seoul, Korea, in 2001 and 2004, respectively.

During his postdoctoral research at the Massachusetts Institute of Technology (MIT) from 2004 to 2006, he was with the Laboratory for Information Decision Systems (LIDS). In 2006, he joined the KHU, where he is currently a Professor in the

Department of Electronic Engineering. His research interests include quantum information science, wireless communication, and machine intelligence.

Dr. Shin received the IEEE Communications Society's Guglielmo Marconi Prize Paper Award in 2008 and William R. Bennett Prize Paper Award in 2012. He served as the Technical Program Co-Chair for the IEEE WCNC (PHY Track 2009) and the IEEE GLOBECOM (Communication Theory Symposium 2012 and Cognitive Radio and Networks Symposium 2016) and the Publicity Co-Chair for the IEEE PIMRC in 2018. He was an Editor of the IEEE TRANSACTIONS ON WIRELESS COMMUNICATIONS from 2007 to 2012 and IEEE COMMUNICATIONS LETTERS from 2013 to 2015.



Moe Z. Win (Fellow, IEEE) is a Professor at the Massachusetts Institute of Technology (MIT) and the Founding Director of the Wireless Information and Network Sciences Laboratory. Prior to joining MIT, he was with AT&T Research Laboratories and with NASA Jet Propulsion Laboratory.

His research encompasses fundamental theories, algorithm design, and network experimentation for a broad range of real-world problems. His current research topics include ultra-wideband systems, network localization and navigation, network interference

exploitation, and quantum information science. He has served the IEEE Communications Society as an elected Member-at-Large on the Board of Governors, as elected Chair of the Radio Communications Committee, and as an IEEE Distinguished Lecturer. Over the last two decades, he held various editorial positions for IEEE journals and organized numerous international conferences. Recently, he has served on the SIAM Diversity Advisory Committee.

Dr. Win is an elected Fellow of the AAAS, the EURASIP, the IEEE, and the IET. He was honored with two IEEE Technical Field Awards: the IEEE Kiyo Tomiyasu Award (2011) and the IEEE Eric E. Sumner Award (2006, jointly with R. A. Scholtz). His publications, coauthored with students and colleagues, have received several awards. Other recognitions include the MIT Everett Moore Baker Award (2022), the IEEE Vehicular Technology Society James Evans Avant Garde Award (2022), the IEEE Communications Society Edwin H. Armstrong Achievement Award (2016), the Cristoforo Colombo International Prize for Communications (2013), the Copernicus Fellowship (2011) and the Laurea Honoris Causa (2008) from the Università degli Studi di Ferrara, and the U.S. Presidential Early Career Award for Scientists and Engineers (2004). He is an ISI Highly Cited Researcher.